FOCUSED ULTRASOUND AND BUBBLE LIPOSOMESCOMBINED TUMOR IMMUNOMODULATION

RAMASAMY SELVARANI,

Bachelor of Veterinary Science,

Tamilnadu Veterinary & Animal Sciences University

Chennai, Tamilnadu, India

2009

Submitted to the Faculty of the
Graduate College of the
Oklahoma State University
in partial fulfillment of
the requirements for
the Degree of
MASTER OF SCIENCE
December, 2017

FOCUSED ULTRASOUND AND BUBBLE LIPOSOMES

COMBINED TUMOR IMMUNOMODULATION

Thesis Approved:

Dr.AshishRanjan

Thesis Adviser

Dr.TomOomens

Dr.PamelaLovern

Name: RAMASAMY SELVARANI

Date of Degree: DECEMBER, 2017

Title of Study: FOCUSED ULTRASOUND AND BUBBLE LIPOSOMES COMBINED TUMOR IMMUNOMODULATION

Major Field: VETERINARY BIOMEDICAL SCIENCES

Abstract:

Background/objectives: It is well-established that the stimulation of immune system of a patient by monoclonal antibodies, adoptive dendritic cell transfer and *in situ* vaccines can enhance antitumoral effects.Despite this, the progression-freesurvival achieved by these methodologies provides amodest improvement over traditional cancer treatment. To overcome these barriers, we hypothesize that focused ultrasound (FU)in combination with bubble liposomes (BL) will induce cellular stress, and elicit micro-environmental changes to induce a potent antitumor response.The objective of the proposed project is to test the feasibility of BL/FU approachagainst colon cancer in vitro and in vivo.

Methods: Mice bearing C26 colon cancer were treated with FUheating and BL. Flow cytometric analysis was conducted to understand thematuration of DCs and macrophages. CytoTox 96® Assay asused to determine T cell-mediated tumor cell lysis.Real-Time gene expression studies were conducted to identify inflammatory cytokines.

Results: FU and BL induceddendritic cell maturation and CTL mediated lysis of tumor cells in vitro. Significantly enhanced infiltration of cytotoxic T-cells in colon tumor was observed 4-fold difference for FU/BL compared to control. Hyperthermia(~42ºC) and BL treatment ofRAW 264.7 macrophages induced an M1phenotype compared to control in-vitro.

Conclusion: Hyperthermia and liposomal nanoparticle treatment induce M1 polarization.FU and BL treatment sensitizes colon carcinoma CT26 cancer cells to the CTLs antitumor response.This technology has the potential for improving immunotherapy response in clinics.

TABLE OF CONTENTS

Chapter Page

LIST OF TABLES

LIST OF FIGURES

CHAPTER I

ROLE OF FOCUSED ULTRASOUND IN CANCER IMMUNOTHERAPY

Cancer Immunotherapy

Solid tumors therapy typically incorporates a combination of surgery, chemotherapy, and radiotherapy in patients. In recent years, the use ofimmunotherapeutic is also gaining prominence as the4thtreatment modality in cancer patients. In this approach, a patient's adaptive immune system is activated to achieve clearance of occult cancerous cells.This is achieved via the : 1) capturing of tumor antigens bydendritic cells (DCs), 2) priming, activation, and expansion of T cells, and 3) T cell trafficking to tumor, and exertion of effector functions (Zhang, Mehta et al. 2008). In general, activation of DCs is first mediated by signals that are released from dying cells (adenosine triphosphate (ATP), high mobility proteins (HMPB1) etc.(Mellman, Coukos et al. 2011). DCs thenendocytose proteins and present peptides on MHC class II molecules for T cell recognition (Rosenberg 1999). T cells sense the tumor cell antigen through T cell receptors (TCR) on thecell surface to drive antitumor immune responses(Dustin, 2016). (Engleman and Fong 2003)(Merad, Sugie et al. 2002) (Mahoney,2015). These mechanisms can be disrupted in asolid tumorsby the suppressor cells (T-regulatory or Tregs), cytokines such as TGF-beta and IL-10 that inhibit dendritic cell (DCs) maturation. Thereby, resulting in tolerance to immune therapy(Inoue, Setoyama et al. 2014). Additionally, the mast cells can aid in the recruitment of T-reg cells in the tumors, and increase angiogenesis; both of which cause tumor growth.Thus, if immune therapy has to succeed, the activation of immune system in vivo must be discretely and precisely controlled (Perica, Varela et al.

2015)(Schuler, Schuler-Thurner et al. 2003). The long term goalof our project is to understand the mechanisms and develop new combinatorial technologies thatsuccessfully remove immunosuppressivemicroenvironment to result in durable survival responses in patients(Hoos, Eggermont et al. 2010).

High Intensity Focused Ultrasound (HIFU) mediated combinatorial therapy

One approach to enhancing immunotherapy can be through combinatorial therapy(Vanneman and Dranoff 2012).For instance, cytotoxic agents aid immunotherapy by activating pro-apoptotic effects in tumor cells via receptor-driven autocrine pathway(Ciardiello, Caputo et al. 2000). However, the use of cytotoxic agents is limited by toxicity and inefficient activation of anti-tumor immunity in a synergistic manner(Mellman, Coukos et al. 2011).In contrast to drug agents,high intensity focused ultrasound (HIFU) energy isa non-invasive and non-ionizing pressure wave delivery technology for thegeneration of mechanical and thermal effects in solid tumors(Tardoski, Ngo et al. 2015). Thermal effects produce cavitation, and non-thermal treatment create a gap between endothelial cells to increase permeability of blood vessels (Husseini and Pitt 2008)(Suzuki, Oda et al. 2009). HIFU immune effects are mediated by genotoxic cell stress and tumor antigen release thattrigger DCs maturation. Matured DCs move to nearby lymph nodes (LNs), and with help from CD4+ T cells stimulate CD8+ T cellsto promote adaptive antitumor immunity (Bandyopadhyay, Quinn et al. 2016)(Hu, Yang et al. 2007)(Clay, Hobeika et al. 2001). HIFU enhances proliferation of a variety of effectors such as monocytes, natural killer cells, and CD4+ helper T cells of type 1 origin(Blattman and Greenberg 2004). In particular,CD4+ T lymphocytes of TH1 originsecrete IFN-γ, and

IL-2. IFN-γ induces macrophages to produce IL-12 to activate cell-mediated immune response. IL-2 increases the viability, and quantity of T lymphocytes to promote anti-tumor activity of CD8 T cells.

Clinical HIFU (0.8–3.5 MH)treatment of tumors (Yang, Reilly et al. 1992)(Hu, Yang et al. 2007) also increase the HSP, HSP72&73, glucose regulated protein GRP75 & 78 ATP, GTP, chromatin protein HMBG1, and calreticulinlevels to increase the infiltration of DCs in tumors (Inoue, Setoyama et al. 2014) (Deng, Zhang et al. 2010).). Specifically, calreticulin interacts with DCs to promote phagocytosis of tumor cells, present tumor antigens on MHC I & II, and release other danger signals (Mellman, Coukos et al. 2011)(Hu, Yang et al. 2007). HIFU also mediate CD4+ non-T reg cells, CD45+ cells (indication for arrival of inflammatory cells), and natural Killer cells (NK cells) activation. Further, the application of HIFU systemically enhances the CD4+ T cells and ratio of CD4+/CD8+ in blood circulation in cancer patients (Wu, Wang et al. 2004).

Current limitations of HIFU technology

Despite the promises of HIFU in solid tumor immune modulation, it has some limitations. A sub-optimal HIFU treatment reduce the level of cytokine production such as vascular endothelial growth factor (VEGF), transforming growth factor-β1 (TGF-β1), transforming growth factor-β2 (TGF-β2), interleukin 6 (IL-6) and interleukin 10 (IL-10) todecrease immune suppressive activity in cancer patients (Zhou, Zhu et al. 2008)(Hu, Yang et al. 2007). HIFU mediated destruction of tissue vascularitycan preventimmune cell infiltration for adaptive antitumor response (Bandyopadhyay, Quinn et al. 2016).Thus, an

appropriate balance between cell viability and cell destruction is critical toachieving specific cytotoxic T-lymphocytes (CTL) against solid tumors.

We hypothesizethat Focused ultrasound combined liposomal treatment of solid tumors can achieve robust immune response and efficacy in vivo. The rationales for this hypothesis stems from the established roles of thermal and mechanical treatment of solid tumors in induction of cell stress, and increased burden of misfolded protein and antigen release. We believe that the liposome uptake by immune cell (macrophage) and tumor cells will disrupt immunosuppressive tumor microenvironment, and reduce acoustic threshold requirements to maximize cellular stress without tumor necrosis. Based on this, the specific aim of our project is:

Aim 1: Investigate the immunomodulatory role of FU and liposome in vitro and in vivo against primary colon tumor (CT26) models

Aim 2:Determine the impact of FU/liposome combinatorial treatment on macrophage polarization in vitro and in vivo

References

Bandyopadhyay, S., T. J. Quinn, L. Scandiuzzi, I. Basu, A. Partanen, W. A. Tome, F. Macian and C. Guha (2016). "Low-Intensity Focused Ultrasound Induces Reversal of Tumor-Induced T Cell Tolerance and Prevents Immune Escape." J Immunol 196(4): 1964-1976.

Blattman, J. N. and P. D. Greenberg (2004). "Cancer immunotherapy: a treatment for the masses." Science 305(5681): 200-205.

Ciardiello, F., R. Caputo, R. Bianco, V. Damiano, G. Pomatico, S. De Placido, A. R. Bianco and G. Tortora (2000). "Antitumor Effect and Potentiation of Cytotoxic Drugs Activity in Human Cancer Cells by ZD-1839 (Iressa), an Epidermal Growth Factor Receptor-selective Tyrosine Kinase Inhibitor." Clinical Cancer Research 6(5): 2053-2063.

Clay, T. M., A. C. Hobeika, P. J. Mosca, H. K. Lyerly and M. A. Morse (2001). "Assays for Monitoring Cellular Immune Responses to Active Immunotherapy of Cancer." Clinical Cancer Research 7(5): 1127-1135.

Deng, J., Y. Zhang, J. Feng and F. Wu (2010). "Dendritic Cells Loaded with Ultrasound-Ablated Tumour Induce in vivo Specific Antitumour Immune Responses." Ultrasound in Medicine & Biology 36(3): 441-448.

Engleman, E. G. and L. Fong (2003). "Induction of immunity to tumor-associated antigens following dendritic cell vaccination of cancer patients." Clin Immunol 106(1): 10-15.

Hoos, A., A. M. Eggermont, S. Janetzki, F. S. Hodi, R. Ibrahim, A. Anderson, R. Humphrey, B. Blumenstein, L. Old and J. Wolchok (2010). "Improved endpoints for cancer immunotherapy trials." J Natl Cancer Inst 102(18): 1388-1397.

Hu, Z., X. Y. Yang, Y. Liu, G. N. Sankin, E. C. Pua, M. A. Morse, H. K. Lyerly, T. M. Clay and P. Zhong (2007). "Investigation of HIFU-induced anti-tumor immunity in a murine tumor model." Journal of Translational Medicine 5: 34-34.

Husseini, G. A. and W. G. Pitt (2008). "The use of ultrasound and micelles in cancer treatment." J Nanosci Nanotechnol 8(5): 2205-2215.

Inoue, S., Y. Setoyama and A. Odaka (2014). "Doxorubicin treatment induces tumor cell death followed by immunomodulation in a murine neuroblastoma model." Experimental and Therapeutic Medicine 7(3): 703-708.

Mellman, I., G. Coukos and G. Dranoff (2011). "Cancer immunotherapy comes of age." Nature 480(7378): 480-489.

Merad, M., T. Sugie, E. G. Engleman and L. Fong (2002). "In vivo manipulation of dendritic cells to induce therapeutic immunity." Blood 99(5): 1676-1682.

Perica, K., J. C. Varela, M. Oelke and J. Schneck (2015). "Adoptive T cell immunotherapy for cancer." Rambam Maimonides Med J 6(1): e0004.

Rosenberg, S. A. (1999). "A new era for cancer immunotherapy based on the genes that encode cancer antigens." Immunity 10(3): 281-287.

Schuler, G., B. Schuler-Thurner and R. M. Steinman (2003). "The use of dendritic cells in cancer immunotherapy." Curr Opin Immunol 15(2): 138-147.

Suzuki, R., Y. Oda, N. Utoguchi, E. Namai, Y. Taira, N. Okada, N. Kadowaki, T. Kodama, K. Tachibana and K. Maruyama (2009). "A novel strategy utilizing ultrasound for antigen delivery in dendritic cell-based cancer immunotherapy." Journal of Controlled Release 133(3): 198-205.

Tardoski, S., J. Ngo, E. Gineyts, J. P. Roux, P. Clezardin and D. Melodelima (2015). "Low-intensity continuous ultrasound triggers effective bisphosphonate anticancer activity in breast cancer." Sci Rep 5: 16354.

Vanneman, M. and G. Dranoff (2012). "Combining immunotherapy and targeted therapies in cancer treatment." Nat Rev Cancer 12(4): 237-251.

Wu, F., Z.-B. Wang, P. Lu, Z.-L. Xu, W.-Z. Chen, H. Zhu and C.-B. Jin (2004). "Activated anti-tumor immunity in cancer patients after high intensity focused ultrasound ablation." Ultrasound in Medicine & Biology 30(9): 1217-1222.

Yang, R., C. R. Reilly, F. J. Rescorla, N. T. Sanghvi, F. J. Fry, T. D. Franklin and J. L. Grosfeld (1992). "Papers presented at the 22nd Annual Meeting of the American

Pediatric Surgical AssociationEffects of high-intensity focused ultrasound in the treatment of experimental neuroblastoma." Journal of Pediatric Surgery 27(2): 246-251.

Zhang, H.-G., K. Mehta, P. Cohen and C. Guha (2008). "Hyperthermia on immune regulation: A temperature's story." Cancer Letters 271(2): 191-204.

Zhou, Q., X.-Q. Zhu, J. Zhang, Z.-L. Xu, P. Lu and F. Wu (2008). "Changes in Circulating Immunosuppressive Cytokine Levels of Cancer Patients After High Intensity Focused Ultrasound Treatment." Ultrasound in Medicine & Biology 34(1): 81-87.

CHAPTER II

FEASIBILITY OF FOCUSED ULTRASOUND AND BUBBLE LIPOSOMES COMBINATION IN-VITRO AGAINST COLON CANCER CELLS

2.1 Abstract

Objective: The objective of this study was to:1. analyze maturation of DCs, and 2. determine T cell-mediated tumor cell lysis with bubble liposome and focused ultrasound against colon carcinoma CT26 cell lines.

Method: Liposomes were synthesized by thin film hydration and extrusion method, and loaded with perfluoropentane (PFP) to generate bubble liposome (BL).CT26 cancer cells were treated with BL and focused ultrasound treatment for 4 min. The supernatant collected from cancer cells was added to dendritic cells, and the maturation was quantified by flow cytometry using CD11c marker. Matured dendritic cells were co-mixed with cytotoxic T cells isolated from spleen of mice. Then, the activated cytotoxic T cells were added to CT26 cells for cytotoxicity assessment usingLDH assay.

Result: Synthesized BL were 160 nm in size.FU/BL enhanced the maturation of dendritic cells by 10-15% compared to controls. A 10-30% increase in CTL cytotoxicity for FU/BL was observed against colon cancer cell compared to controls.

Conclusion:FU/BL combination sensitizesthe CTLsagainst C26 cancercells in vitro.

2.2 Introduction

Currently, advanced colon carcinoma cancer has poor 5-year survival rates. To enhance therapeutic outcomes, the objective of this study was to combine FU with bubble liposomes for induction of cytotoxic T-lymphocytes (CTL) mediated anti-tumor immune response against colon cancer in vitro. Focused ultrasound generates acoustic radiation forces and acoustic cavitation in tumor tissues(Liu et al. 2012). Such forces induce low-level mechanical stress and mild hyperthermia (40-45°C), possibly resulting in membrane perturbation without causing significant thermal injury or cell death. The biological effects of focused ultrasound (FU) and its effect on CTL with liposomal gas bubbles are yet to be demonstrated. We hypothesized that combinational treatment of focused ultrasound (FU) and bubble liposomes (BLs) will exert synergetic antitumor cancer effect by stimulating maturation of dendritic cells activation of tumor-specific CTLs (Pei, Pan et al. 2015). To do so, theC26 antigens specific cytotoxic T cells were targeted against colon cancer cells to understand specific antitumor immune response.

2.3 Materials and methods

2.3.1 Reagents

DPPC, 1, 2-Dipalmitoyl-sn-glycero-3-phosphocholine (LP-R4-057), MPEG-2000-DSPE (LP-R4-039). S-lyso-PC, 1-Stearoyl-2-lyso-sn-glycero-3-phosphocholine (LP-R4-083) lipids were purchased from cordon pharma (USA). Recombinant granulocyte/macrophage colony stimulating factor (GM-CSF) was obtained from R&D Systems (Minneapolis, MN, USA). Fluorescein isothiocyanate (FITC)-conjugated CD11c were obtained from eBioScience (Bedford, MA, USA). Mojosort mouse CD3 T cell

isolation kit, APC anti-mouse CD3e,PE anti-mouse CD4, FITC anti-mouse CD8a, PE/Cy7 anti-mouse IL-2, PerCP/Cy5.5 anti-mouse IFN-g (BioLegend,USA) were purchased from Biolegend.

2.3.2 Synthesis of bubble liposomes (BLs)

Liposomes were synthesized as described previously (Danny Maples et al., (2015). Briefly, the phospholipids (MSPC, DPPC, and DSPE-mPEG2000) were dissolved in a minimum amount of chloroform ($CHCl_3$) at a molar ratio of 85.3:9.7:5.0. The solvent was evaporated and the resulting lipid film was hydrated in citrate buffer (pH 4.0) mixed with 1,3-propanediol (PD; 0.65M) at 55 °C and extruded five times through double-stacked 200 nm polycarbonate filters to yield a final lipid concentration of 50 mg/mL. A PD-10 size-exclusion column equilibrated with 5–10 column volumes of 1x phosphate buffer saline (PBS) was used to remove free 1,3-PD from the outside of the liposomes. Bubble liposomes was prepared by loading liposomes with Perfluoropentane (99%, Exfluor Research Corporation, Texas, USA) as the bubble agents using a one-step sonoporation method. Briefly, 2 mL of the liposomal formulations were incubated under continuous sonication (~20 khz) in 3 mL vials along with PFP (boiling point 30°C; 20 µL/100 mg lipid) for 1–2 min. PFP and liposomes were kept cold prior to being combined, and the sonication bath was kept at 4°C to minimize PFP vaporization. Free PFP was removed by column purification. This method was repeated at least in triplicate (n = 3) for evaluation.Liposomes (LTSLs and BLs) were characterized for size (z-average) using a dynamic light scattering (DLS) instrument (Zetapals, Brookhaven Instruments Corporation)

2.3.4 Cell culture

C26 cells were provided by the National Cancer Institute kindly provided.The cells were cultured in Roswell Park Memorial Institute medium 1640 medium (RPMI, containing 2 mmol/L L-glutamin,10 mmol/L HEPES,100 U/mL penicillin, and 100 mg/mL streptomycin) supplemented with 10% fetal calf serum (FCS, Wisent Inc., Saint-Jean-Baptiste, QC, Canada).

2.3.5 FU therapy in thin walled PCR tubes

Prior to HIFU treatment, $2*10^5$ cells in 200µL media were gently transferred in a 0.5 mL thin-walled PCR tube, and placed vertically with its conical bottom aligned within the beam focus of the HIFU transducer as described previously by Hu et al.2012 Ultrasound exposures were delivered to the tube on a singlespot for 240seconds. HIFU transducer had1.5 MHz central frequency, 45 mm radius and 64 mm aperture diameter with central opening 40 mm in diameter. The therapeutic ultrasound device was operated in continuous-wave mode at a specific acoustic power: acoustic power 15W, PRF 1Hz, duty cycle 10% to provide non-ablative FU (Liu, Hsieh et al. 2012). Following the treatment, cellswere centrifuged for 5 minutes at 250 G, and the supernatant PBS was harvested for further analysis.

2.3.6 Generation of dendritic cells from bone marrow derived cells

Bone marrow–derived cells were harvested from the femur and tibia of C57BL/6 mice and cultured in RPMI 1640 medium supplemented with 10% FBS in the presence of 20

ng/mL murine GM-CSF (R&D). Loosely adherent immature dendritic cells were harvested after 6 days of culture as described previously(Madaan, Verma et al. 2014).

2.3.7 Confirmation of maturation of DCs by confocal microscopy

C26 supernatant was added to the dendritic cells on day 6 post treatment. After 24h of treatment, the cells were transferred into 35mm MatTek well plate for 60x oil immersion confocal microscopy (Tan, Leong et al. 2010). All imaging was performed with constant acquisition and display parameters using an inverted microscope (Olympus IX81-ZDC2) equipped with a color CCD camera, cooled monochrome CCD camera, motorized scanning stage, and mosaic stitching software (Metamorph) with a 60x oil-immersion objective.

2.3.8 Flow cytometry analysis for maturation of DCs

CD11c was used as a marker of DC maturation. Briefly, the DCs were harvested in complete medium at 37°C, 5% CO_2. The samples were analyzed on FACs Aria flow cytometer using BD FACSD via 8.0.1 software (Kim and Diamond 2007). The percentage of cells positive for binding was computed from the histogram plot calculated from triplicate measurements of each sample. Ten thousand single cell events were counted from each sample.

2.3.9 Lactic dehydrogenase (LDH) cytotoxicity assay

CytoTox 96 Nonradioactive Cytotoxicity assay (Promega; Madison, WI, USA) was used to determine T cell-mediated tumor cell lysis. Target cells were harvested washed, and

50 µL/well was plated in a 96-well plate. T-cells pulsed with DCs were added at different effector: target cell(C26 cells) ratio of 1:10, 1:5, 1:2.5 for 4 hours, at 37 C. 50µL of supernatants were harvested and measured for LDH activity following the manufacturer's protocol. Controls for spontaneous LDH release in effector and target cells, as well as target maximum release, were prepared simultaneously. Cytotoxicity assay (%) was calculated by the formula:

(Experimental-Effector Spontaneous-Target Spontaneous) / (Target Maximum-Target Spontaneous) *100.

2.3.10 Statistical analysis

The results were analyzed using Graphpad6.0 (GraphPad Software Inc.). Multiple groups were analyzed by analysis of variance (ANOVA) followed by pairwise comparison. $P<0.05$ was considered statistically significant. Data are expressed as mean ± standard deviation (SD).

2.4. Results

2.4.1 Validation of size and zeta potential for BL

The hydrodynamic diameter of BL was 160nm size and zeta potential was -48.95mV (Fig 1 and Table 1). The synthesized BLs was stable in an aqueous environment and exhibited no visual evidence of particle accumulation at the time of treatment**.**

2.4.2 Combination of FU and BL stimulated the maturation of DCs

FU or BL alone caused ~ 5%, and FU/ BL combination induced ~8-10% maturation of DC, and these were significantly greaterthan the control (Fig 4 and Table 2). These findings were confirmed by the confocal microscopic studies where an extended dendrites on matured dendritic cells compared to the non-matured cells was noted (Fig. 3).

2.4.3 Combination of FU and BL stimulated C26 cell specific CTL antitumor response

CTLs co-incubated with C26 supernatant treated DCs were added to C26 cancer cells in a 1 in 10 ratio to assess their activation status and tumor cell killing ability. FU+BL combination resulted in 40% killing of C26 cancer cells by the CTLs (> 4-fold than the control; Fig. 5). FU and BL alone did not significantly enhanced tumor cell killing.

2.5 Discussion

Colon cancer is the third leading cause of death in cancer patients. It is poorly responsive to the conventional therapies due to the aggressive and invasive properties. These tumor cells have immune suppressing and escape mechanisms and respondpoorly to chemotherapy, and radiotherapy. The activation of immune cells namely dendritic cells which form the bridge between the innate and the adaptive immunity and cytotoxic T lymphocytes which have the tumor cell killing ability can complement the current limitation of conventional anticancer treatments approaches. The objective of this study was to assess the ability of FU+BL combination to generate

C26 specific cytotoxic T cell mediated response in vitro. We developed BL by film hydration technique which resulted in about 150-170 nm sized homogeneous unilamellar population. Importantly, the encapsulation of the bubble agent did not affect the stability of the liposomes up to 24 hours. Treatment of C26 tumor cells with FU+BL likely induced thesecretion of soluble antigens. This was evidenced by an ability of cell supernatants to activate dendritic cells by ~5-10% compared to untreated controls (Fig. 3 and 4). Additional studies on methods determine the specific soluble antigens released from the tumor cells after FU+BL therapy can shed more light on the signaling molecules involved in this process. Regardless, the T-cell activated with the supernatants from FU+BL therapy stimulated cytotoxic killing of C26 cells. The ability of cytotoxic T cells to kill tumor cells was assessed by lactate dehydrogenase assay (LDH). LDH is a cytosolic enzyme that is release in to the media from damaged cells as biomarker for cellular cytotoxicity and cytolysis. While the presence of FU or BL alone did not cause any significant change in tumor cell killing ability of cytotoxic T cells, co-incubation of the FU/BL activated T cells caused significant tumor cell killing (Fig. 5). Thus, our in vitro data suggest thetheBL/FU combinatorialtherapy may hold potential as an adjuvant to modulate immune response in cancer medicine.

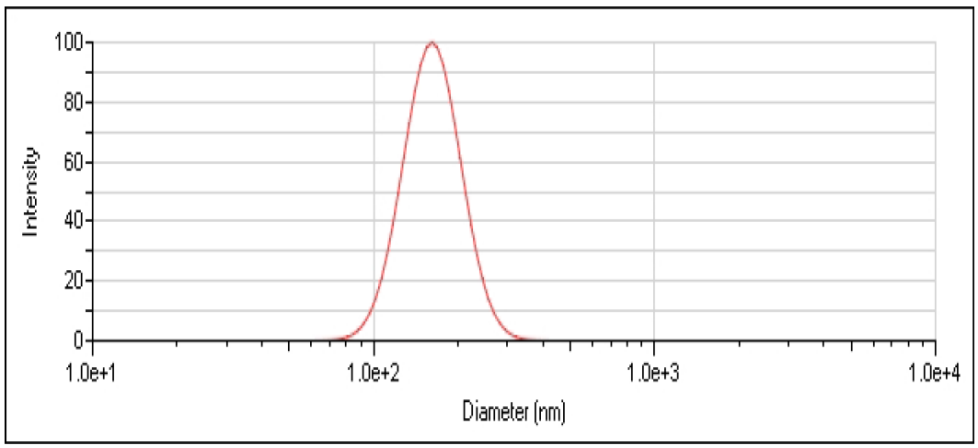

Fig 1: BL size analysis in DLS.

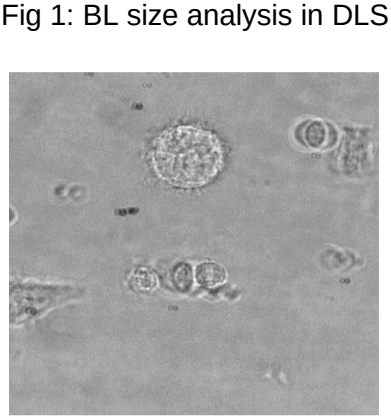

Fig 2: Confocal microscopy showing mature DCs under confocal microscopy

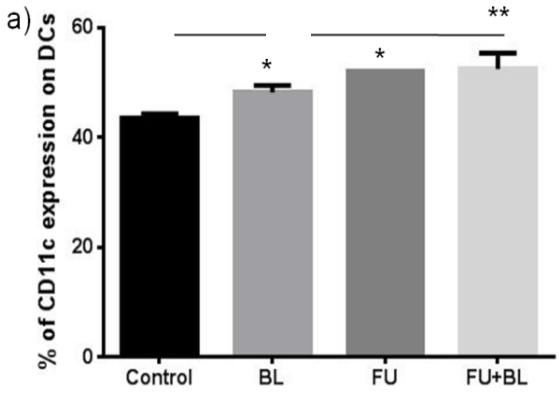

Fig 4: Flow cytometry evaluation ofdendritic cell maturation following treatment with FU, BL, and BL/FU

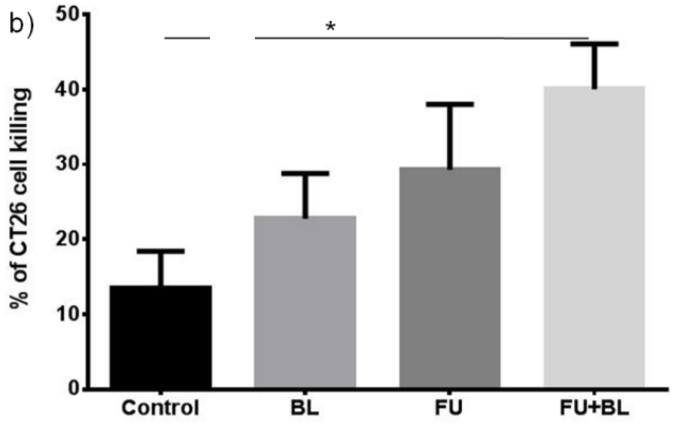

Fig 5: CTL-mediated colon cancer celllysis. Significantly enhanced killing of cancer cells was noted with FU/BL combination.

Table 1. Size, polydispersity and zeta potential of BL at 25°C

Liposome	**Size (nm)**		**Polydispersity**		**Zeta potential (mV)**	
	mean	SD	mean	SD	mean	SD
BL	160.16	1.14	0.092	0.038	-48.96	1.96

2.6 References

Kim, S. J. and B. Diamond (2007). "Generation and maturation of bone marrow-derived DCs under serum-free conditions." J Immunol Methods 323(2): 101-108.

Liu, H. L., H. Y. Hsieh, L. A. Lu, C. W. Kang, M. F. Wu and C. Y. Lin (2012). "Low-pressure pulsed focused ultrasound with microbubbles promotes an anticancer immunological response." J Transl Med 10: 221.

Madaan, A., R. Verma, A. T. Singh, S. K. Jain and M. Jaggi (2014). "A stepwise procedure for isolation of murine bone marrow and generation of dendritic cells." Journal of Biological Methods 1(1).

Maples, D., K. McLean, K. Sahoo, R. Newhardt, P. Venkatesan, B. Wood and A. Ranjan (2015). "Synthesis and characterisation of ultrasound imageable heat-sensitive liposomes for HIFU therapy." Int J Hyperthermia 31(6): 674-685.

Pei, Q., J. Pan, X. Ding, J. Wang, X. Zou and Y. Lv (2015). "Gemcitabine sensitizes pancreatic cancer cells to the CTLs antitumor response induced by BCG-stimulated dendritic cells via a Fas-dependent pathway." Pancreatology 15(3): 233-239.

Tan, Y. F., C. F. Leong and S. K. Cheong (2010). "Observation of dendritic cell morphology under light, phase-contrast or confocal laser scanning microscopy." Malays J Pathol 32(2): 97-102.

CHAPTER III

FOCUSED ULTRASOUND AND BUBBLE LIPOSOMES IMMUNOMODULATION IN MOUSE COLON CANCER

3.1 Abstract

Background: Focused ultrasound can exert thermal ablation, acoustic cavitation, and immunomodulation. We hypothesize that immunomodulation with sub-lethal mild hyperthermia and Bubble liposomes (BL) will increase cross presentation of tumor antigens by DCs and activation of tumor-specific CTLs. The objective of this study was to investigate BL/hyperthermia combination in a mouse model of colon cancer.

Methods: Thermometry during focused ultrasound treatment was estimated by inserting a temperature sensor in a vial plus/minus BLs. C26 tumors was subcutaneously induced in the thigh region of mice. BL were administered intravenously, and 4min HIFU treatment were administered with Alpinion HIFU system. The ratio of CD4+/CD8+ cells in tumor and volume were analyzed on day 10-post treatment.

Results: Results indicated an average 1°C temperature risein BL containing tube compared to FU treatment alone. Both FU and FU + BL delayed tumor growth compared the other treatment groups, however, FU survival rates were not different than FU/ BL combination.

Conclusion: Our animal study demonstrated that FU or FU/BL induces systemic immune response compared to control group.

3.2 Introduction

HIFU temperature exposure cause HSP70 expression and misfolded protein synthesis in the tumor cells (Guha et al. 2012). However, it is not clear whether the adaptive immune responses can be impacted with increasing temperatures (Bandyopadhyay, Quinn et al. 2016). There is some evidence that IFN-γ secreting T cells areinduced in relatively higher numbers with non-thermal mechanical HIFU than thermal treatment. The mechanical and thermal effects of HIFU therapy can be controlled by optimizing the HIFU parameters such as pulse duration time, pulse repetition rate, number of pulses, and transducer voltage. The objective of this study was to optimize the HIFU parameters and understand the mechanism of mechanical and thermal treatment of colon tumors on the immune cell infiltration (CD3+, CD4+, CD8+, IFN-y, IL-2) in blood and tumors2-3 weeks after treatments.

3.3 Methods

3.3.1 Optimization of FU for mechanical and thermal effects

200uL of water, and E-LTSL was transferred into a PCR tube and exposed to focused ultrasound treatment. During treatment, temperatures in the vials were measured with T-type thermocouples(diameter 200μm)(Watanabe, Kakuta et al. 2005). Temperature was recorded for ~5 min.and was repeated six times. Then, the mean increase in the temperature wasanalyzed.

3.3.2 Generation of mouse tumor model in Balb/c mice

C26 cell lines cultured in a 75cm^2 flask to 80-90% confluence wastrypsinized with 2mL trypsin. After 2-3 min of trypinization, 4-5mL of complete RPMI was added to the cells, and the cell suspension was transferred to a 15mL tube and centrifuged at 1000 rpm for 10 minutes at 4ºC. The supernatant was discarded and 10 mL of ice cold PBS added to the cell pellet and centrifuged. The cells were suspended into PBS by gentle pipetting. The cell viability was determined by trypan blue staining. The number of cells was determined using a hemocytometer as given below:

No. of cells per mL = $(\text{cell count from four chamber}/4) * 2 * (10^4)$

2 is the dilution factor (1:1 trypan blue dilution)

Basedon the cell count, the cell pellet was diluted with PBS to achieve a final concentration of 0.5*10^6 cells/50uL. Next, Balb/c mouse was inoculated with 50uL injection of the single cell suspension (0.5*10^6/50uL) in the right flank region.

3.3.3 FU+BL treatment

FU was targeted into the center of tumorfor 240 seconds following BL injection (100µL; 40ug/mL concentration) Acoustic coupling was provided by degassed water. The therapeutic ultrasound device was operated in continuous-wave mode using the following parameters: 1)Mechanical focused ultrasound (MOFU):acoustic power: 15W, PRF: 1Hz, duty cycle: 10%; 2) Thermal focused ultrasound (TOFU): acoustic power: 15W, PRF: 1Hz, duty cycle: 10%.Control groups includedSaline, BL, MOFU, TOFU,

MOFU+BL, and TOFU+BL.Tumor bearing mice were monitored tumor volumesupto 21 days.

3.3.4 Samplecollection and processing for flow cytometry

Blood was collected in EDTA tubes from mice by cardiac puncture (10uL of 0.5 M EDTA for 1mL of blood). The blood was diluted 2-fold with PBS. Next,Ficoll solution was added to thediluted blood, mixed, and centrifuged at 800 g for 30 minutes at 25º C. The cell layer at the interface between PBS and Ficoll solution was collected for isolation of CD3+ cells. The cell layer was washed with 0.5mL of PBS containing 2% BSA & 2mM EDTA. In contrast to blood, the harvested tumor werechopped into < 3mm pieces, suspended in 5 mL of dissolution solution containing RPMI with 5% FBS and 300uL of collagenase (200 U/mL) type I (Roche Diagnostics, Germany) and incubated at 37 °C for 30 min. The suspension was vortexed every 10 min during the incubation. After incubation, the cell suspension was passed through a 70 µm cell strainer (Falcon, USA) and centrifuged for 300G for 5 minutes. The supernatant was discarded, and the cells were processed further for flow analysis.

3.3.5 CD3 T cell Isolation

The cells from 3.3.4 was incubated with Biotin-antibody cocktail containing Biotin Ly6G/Ly6C (Gr1), CD45R/B220, CD49b, CD19, CD11b, CD24, TER119/ Erythroid (10 µL of antibody cocktail for $1x10^7$ cells in 100 µL of PBS)for 15 min inice. Then, Streptavidin nanobeads (10 µL of streptavidin nanobeads for 1x107 cells in 100 µL of PBS) were added and the cells were incubated for 15 minutes on ice. Next, PBS was

added to the above cell suspension and kept in amagnet for 5 min. The magnetically labeled non $CD3^+$ T cell fraction was isolated using the magnetic separator, and finally the$CD3^+$ T cells were collected by decanting the liquid in a clean tube.

3.3.5 Staining of samples with antibody for flow cytometry analysis

The CD3+ cells isolated from blood and tumor were labelled with CD3+ antibody APC (5uL of 0.2 mg/mL for $1*10^6$ cells in 100uL). This cell suspension was split into three tubes for labelling with different antibodies as follows: Tube1: CD4+ and CD8+, Tube2: IL-2 and IFN- γ; Tube 3: CD3+ as a control. Briefly, CD4+ PE (5µL of 0.2 mg/mL for 1*106 cells) and CD8+ (1uL of 0.5 mg/mL for 1*106 cells) antibodies were added to the Tube 1, vortexed and mixed well. This suspension was centrifuged at 300 G for 5 min. The supernatant was discarded. The cell pellet was washed with 500 µL of PBS and re-suspended in 500 µL of PBS for flow cytometry analysis. For labelling with IL-2 and IFN-γ antibodies, the CD3+ cell suspension in the Tube 2 was fixed with twice the volume of 4% Paraformaldehyde for 15 min, and centrifuged at 300G for 5 minutes. The supernatant was removed, and the cell pellet was incubated in 500µL permeabilization buffer for 5min, centrifuged at 300G for 5 minutes, and supernatant was discarded. At this step, 0.65 µL of 0.2 mg/mL of IL-2 and 0.5 µL of 0.2 mg/mL of IFN- γ antibodies were added to the cell pellet, kept for 15 min incubation at room temperature, centrifuged at 300G for 5 minutes. The cell pellet was washed with 500 µL of PBS and re-suspended in 500 µL of PBS for flow cytometry analysis. Samples were analyzed usingFACS Aria flow cytometer. Data acquisition was done using BD FACSD via 8.0.1 software.

3.3.7 Statistical analysis

The results were analyzed using Graphpad6.0 (Graph Pad Software Inc.). Multiple groups were analyzed by analysis of variance (ANOVA). $P<0.05$ was considered statistically significant. Data are expressed as mean ± standard deviation (SD).

3.4 Results

3.4.1 Optimization of FU parameters

FU parameters caused no change in temperature with mechanical MOFU.TOFU treatment increased temperatures by 42- 45 °C in thetubes (Fig.7). Increase in temperature was power dependent. A 6-9 °C elevation in temperature was observed following an increase from 6 to10-12.5 W.

3.4.2 Immunomodulation of tumors with FU+BL

MOFU alone didn't impact the CD4+/CD8+ ratio in tumor and blood, and MOFU/BLincreased the ratio by 2-fold in the blood. In contrast, thermal focused ultrasound(TOFU+BL) showed a modest increase (~0.5 fold) in CD+/CD8+ ratio compared to saline treated. In all treatments,IFN-y and IL-2 level blood levels weresignificantly altered compared to theuntreated control (Fig. 9).

3.4.3. Tumor volume

Mice were dived into 6 groups. 1)Saline 2)BL 3)MOFU 4)MOFU+BL 5)TOFU 6)TOFU+BL. Tumor volumes were measured thrice weekly using Vernier calipers along with physical activity. Our treatment group mice MOFU, MOFU+BL, TOFU,T OFU+BL

showed 500mm^3, 450 mm^3, 680 mm^3, 550 mm^3 respectively (Fig. 8). Tumor volumes were taken over 21 days, and calculated through formula V=L*W*W/2, where V is tumor volume, W is tumor width, L is tumor length and it showed reduction in tumor growth compared saline control group.

3.5 Discussion

Here we compared MOFU and TOFU immune effects in colon cancer. MOFU didn't increase temperature, and likely was non-cytotoxic in vivo. In contrast, TOFU caused 42-45°C temperature elevation with the selected HIFU parameters. In prior research,Saha et al demonstrated that low intensity focused ultrasound reduced tumor growth significantly in mice model(Saha, Bhanja et al. 2014). However, our study suggests that the BL/FU effects is immunomodulatory, but do not significantly impact survival responses.

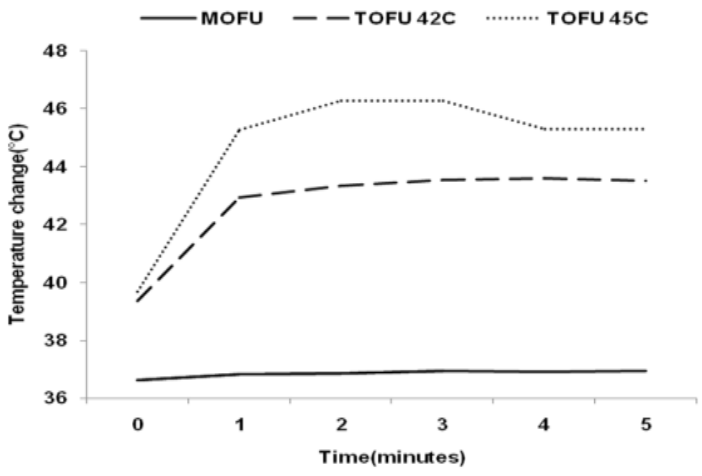

Fig 7: MOFU and TOFU induced temperature changes in PCR tubes containing water.

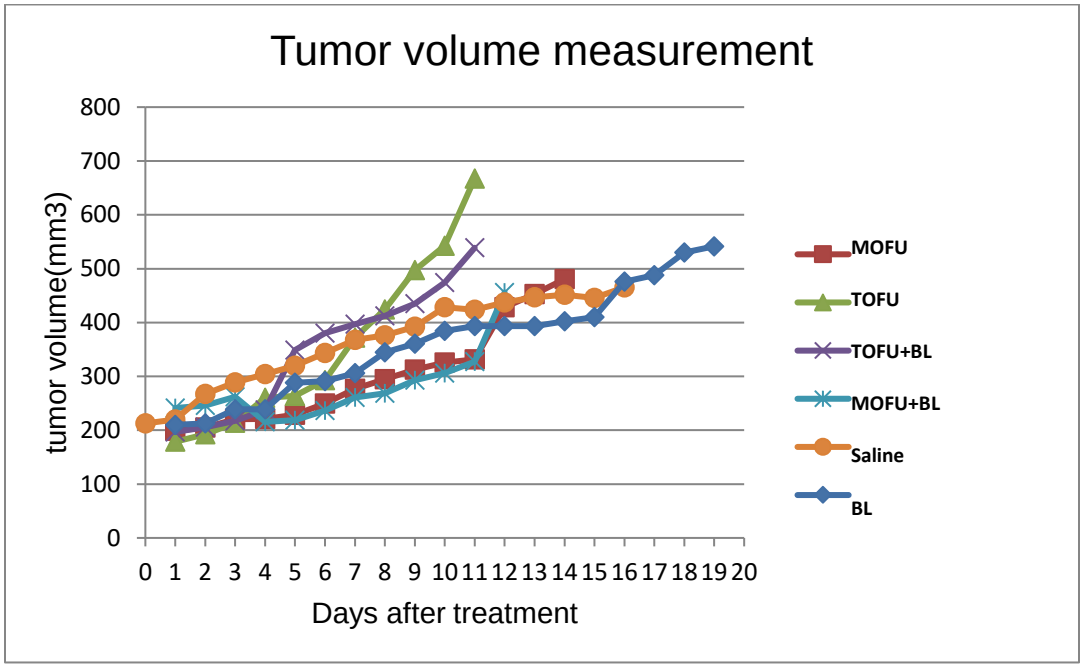

Fig 8: Tumor volume measurement for 21 days.

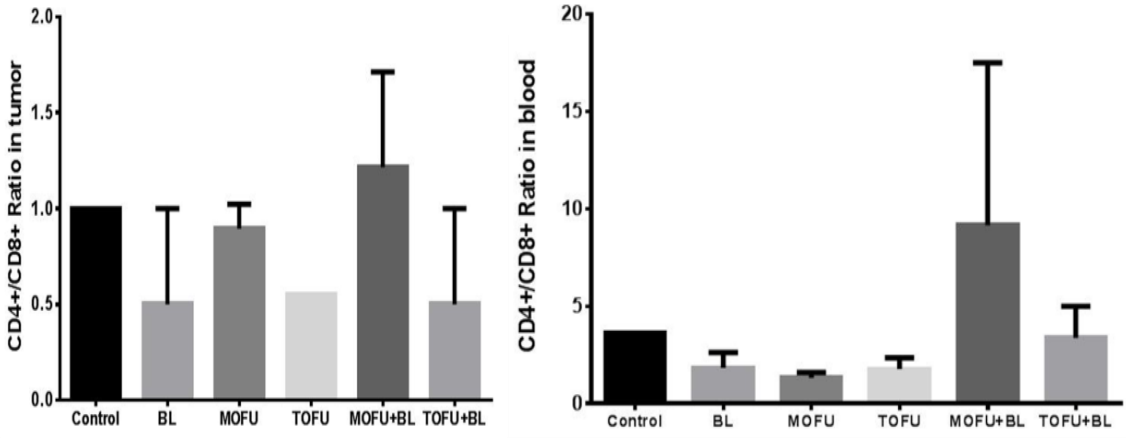

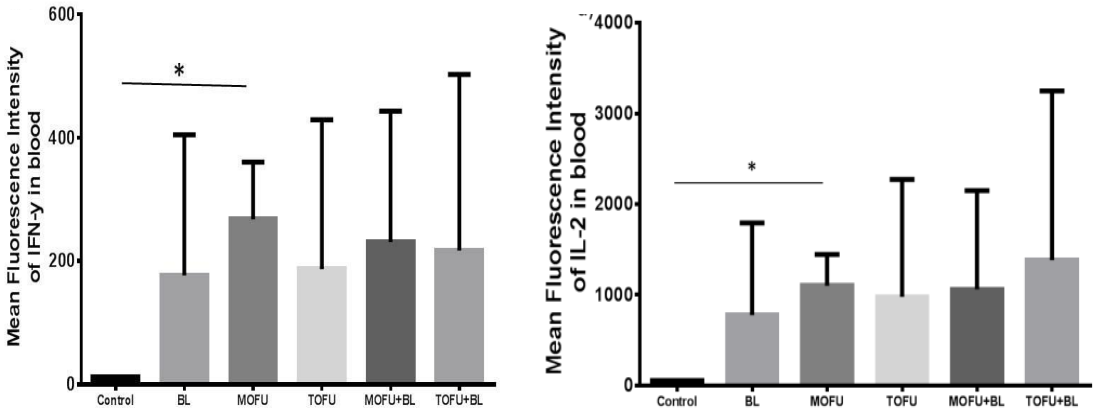

Fig 9: Flow cytometry analysis of CD4+, CD8+, IFN-y and IL-2

3.6.References:

Bandyopadhyay, S., T. J. Quinn, L. Scandiuzzi, I. Basu, A. Partanen, W. A. Tome, F. Macian and C. Guha (2016). "Low-Intensity Focused Ultrasound Induces Reversal of Tumor-Induced T Cell Tolerance and Prevents Immune Escape." J Immunol 196(4): 1964-1976.

Hu, Z., X. Y. Yang, Y. Liu, G. N. Sankin, E. C. Pua, M. A. Morse, H. K. Lyerly, T. M. Clay and P. Zhong (2007). "Investigation of HIFU-induced anti-tumor immunity in a murine tumor model." J Transl Med 5: 34.

Saha, S., P. Bhanja, A. Partanen, W. Zhang, L. Liu, W. Tomé and C. Guha (2014). "Low intensity focused ultrasound (LOFU) modulates unfolded protein response and sensitizes prostate cancer to 17AAG." Oncoscience 1(6): 434-445.

Watanabe, M., N. Kakuta, K. Mabuchi and Y. Yamada (2005). "Micro-thermocouple probe for measurement of cellular thermal responses." Conf Proc IEEE Eng Med Biol Soc 5: 4858-4861.

Zhou, Q., X.-Q. Zhu, J. Zhang, Z.-L. Xu, P. Lu and F. Wu (2008). "Changes in Circulating Immunosuppressive Cytokine Levels of Cancer Patients After High Intensity Focused Ultrasound Treatment." Ultrasound in Medicine & Biology 34(1): 81-87.

CHAPTER IV

LIPOSOME AND HYPERTHERMIA TREATMENT OF MACROPHAGES INDUCES AN M1 POLARIZATION

4.1 Abstract

Background: Demonstration of the intrinsic impact of lipid nanomaterial uptake on macrophage polarization mechanisms can broaden their application for immunotherapeutic applications. Also, its combination with hyperthermia treatment (40-45ºC) will provide new insights on the potential of combinatorial immunotherapies

Methods: Liposomes were prepared by hydration of lipid film followed by the extrusion method and hyperthermia treatment of macrophage cell was performed using a water bath method as described previously. Flow cytometry analysis for CD86 and Cd206 and gene expression analysis were performed for pro-inflammatory (IL1-beta, TNF-α, IL6) and anti-inflammatory (IL10) cytokines.

Results: Results indicated that the CD86 protein expression was 3%, 30% and 10% for control, heat and liposome + 42°C, liposome + 45°C respectively. In contrast, the expression of CD206 increased by 1% compared to untreated controls

Conclusion: our novel concept of liposome combined hyperthermia therapy of macrophages provides new insights on ways to spatially control the macrophage polarization and plasticity within tumors.

4.2. Introduction

The use of body's own immune system to target cancerous cells is rapidly emerging as an important modality for cancer prevention and treatment. Immune-mediated targeting of cancerous cells includes various strategies such as adoptive transfer of activated T-cells, vaccines, or the removal of the immunosuppressive environment in the solid tumor(Farkona, Diamandis et al. 2016). A variety of inflammatory cells including tumor-associated macrophages (TAMs), myeloid derived suppressor cells, and lymphocytes have been linked to tumor immunosuppression. Of these, TAMs are the most abundant inflammatory cells of the tumor microenvironment, amounting to 50% of the tumor mass. TAMs are present at all stages of tumor progression and can be classified into two phenotypes: M1 (classical activated) and M2 (alternatively activated pro-tumor) (Zhou, Zhang et al. 2017). In a solid tumor, TAMs demonstrating an M2-like phenotype has shown to cause invasion, metastasis, drug resistance and the emergence of cancer stem cells (Mielgo and Schmid 2013). Alternatively, the activation and recruitment of M1 macrophages were found to correlate well with antitumor immunity and improvement in the therapeutic efficacy of chemotherapeutics through reduction of drug resistance (especially in pancreatic and lung tumors) (Beatty, Chiorean et al. 2011, Yuan, Hsiao et al. 2015). Thus, the reprograming and enhanced infiltration of TAMs with an M1 phenotype or induced expression of M1 gene or cell surface proteins in tumor microenvironment can be a critical step in improving response to therapy in solid cancer.

We hypothesized that the macrophage phenotype can be modulated by nanoparticle uptake and hyperthermia (40-45ºC) treatment. The motivation for this idea stemmed from recent observation of an induction of pro-inflammatory immune response with an M1 phenotype following phagocytosis of iron-oxide nanoparticles (Mayer, Dougherty et al. 1997, Miller, Zheng et al. 2015). What is not known is whether the M1 induction is strictly dependent on iron-oxide phagocytosis by the macrophages, or occurs independently of nanoparticle particle chemistry.To address this question, our objective was to perform a comprehensive analysis of macrophage polarization mechanism following hyperthermia/liposome treatment. Although multiple types of nanoparticle (NP) platforms (iron oxide, silica, gold, silver, polymers, liposomes etc.) are currently under development, and each has a unique profile of advantages, limitations, we chose liposomes to investigate our hypothesis for multiple reasons. The physical properties and tumor drug-delivery capabilities of stealth and thermosensitive liposomes have been well-characterized in patients (Allen and Cullis 2013, Arranja, Pathak et al. 2016). Long circulating PEGylated stealth liposomes (e.g. Doxil) accumulate selectively in extravascular spaces of tumors to enable slow drug release via enhanced permeability and retention (EPR) mechanisms(Drummond, Meyer et al. 1999, O'Brien, Wigler et al. 2004, Manzoor, Lindner et al. 2012, Gonzalez-Martin and du Bois 2016), while systems such as low temperature-sensitive liposomes (LTSL) enable triggered release of drugs within tumor blood vessels at hyperthermia range temperatures mildly elevated above normal body temperature (>40°C)(Boissenot, Bordat et al. 2016). Thus, liposomes are excellent nanocarrier for drug delivery. Additional demonstration of the intrinsic impact of lipid nanomaterial uptake on macrophage polarization mechanisms

can broaden their application for immunotherapeutic applications. Also, its combination with hyperthermia treatment (40-45ºC) will provide new insights on the potential of combinatorial immunotherapies (Zanganeh, Hutter et al. 2016). Data suggest that liposome/hyperthermia treatment impacts macrophages physiology, and this phenomenon can assist with novel nano immunotherapeutic development.

4.3 Material and methods

4.3.1 Synthesis of liposomes

Lipids were prepared by hydration of lipid film followed by the extrusion method described previously(Senavirathna, Fernando et al. 2013). Briefly, three phospholipids (MSPC, DPPC, and DSPE-mPEG2000) were dissolved in a minimum amount of chloroform ($CHCl_3$) at a molar ratio of 85.3:9.7:5.0. The solvent was evaporated and the resulting lipid film was hydrated in phosphate buffered saline (PBS) at 55°C and extruded five times through double-stacked 200 nm polycarbonate filters to yield a final lipid concentration of 50 mg/mL. A PD-10 size-exclusion column equilibrated with 5–10 column volumes of 1x phosphate buffer saline (PBS) was used to remove free 1,3-PD from the outside of the liposomes.

4.3.2 Characterization of liposomes

Liposome was characterized for size, polydispersity index and zeta potential using a dynamic light scattering (DLS) instrument (Brookhaven Instruments, Holtsville, NY). Briefly, samples were diluted by adding 20 µL of liposomes to 1.5mL of PBS or

deionized water in a cuvette, and an average of three measurements was taken to determine the mean size (± SEM) and zeta potential of the nanoparticles.

4.3.3 Cell Culture

RAW 264.7 macrophages were grown in tissue culture flasks using Dulbecco Modified Eagle Medium (DMEM) cell culture medium supplemented with 10% fetal bovine serum (FBS) and 1% penicillin–streptomycin at 37°C with 5% CO_2 in an incubator. Macrophages were harvested at 70–90% confluency, and seeded a rate of $1x10^6$ cells/2 mL onto 6 well cell culture plates. Prior to the experiment, the culture medium was discarded and cells in the wells were incubated with fresh serum free DMEM medium. Likewise, B16F10 cells were grown in DMEM supplemented with 10% FBS and 1% penicillin–streptomycin at 37°C with 5% CO_2 in an incubator for MTT assay.

4.3.4 Hyperthermia set-up for cell exposure

Hyperthermia treatment of macrophage cell was performed using a water bath method as described previously (Tagami, Ernsting et al. , Kong, Anyarambhatla et al. 2000). After receiving liposome treatment for 15 minutes, the culture plates containing $1x10^{6\ RAW}$ 264.7 macrophage cells/well were placed in a water bath set to ~37, 42, and 45°C for 15min.Rise in temperature during hyperthermia treatment was confirmed by placing a fiber-optic temperature sensor in the water bath. Upon completion of hyperthermia treatment, culture plates were returned to 5% CO2 incubator at 37°C for efficacy or macrophage polarization studies.

4.3.5 Cytotoxicity assessment of heat against macrophages

An in-vitro homogeneous, colorimetric method for determining the number of viable cells using the MTT Non-Radioactive Cell Proliferation Assay (Promega, USA) was used to determine any cytotoxic effects of LTSL upon hyperthermia treatment. Briefly, ~10 x 10^3 cells suspended in 100 µL of DMEM were seeded in 96-well plates and incubated for 24 hours at 37°C in a 5% CO_2 atmosphere following treatment with liposomes at an equivalent dose of 10µM of Dox at 37, 42, and 45°C for 15min along with untreated control. Following this, the culture media was discarded, and the cells in each well were washed with PBS and re-suspended with 100 µL of cell culture media. Then 10 µL of MTT reagent solution was pipetted into each well, and the plates were incubated for 4 hours at 37°C in a humidified 5% CO_2 atmosphere. The absorbance at 540 nm was recorded using a 96-well Elisa plate reader.

4.3.6 Confocal Microscopy of liposome uptake

To confirm liposome uptake of macrophages, a fluorescent methodology was developed. Briefly, a thin film of LTSLs (lipid composition: DPPC, MSPC, DSPE-mPEG2000, and Coumarin-6 at a molar ratio of 84.3:9.7:5:1) was prepared as described in section 2.2 and hydrated and extruded with 2 mL of PBS for 15–30 min at 55°C. Prior to the experiment, 1 x 10^6RAW 264.7 macrophage cells in matTek well plate 10-mm diameter microwells of 35-mm petridishes (MatTek Corporation, USA). were washed with 1 mL of PBS, added with 6uL/well of fluorescent liposomes (matching a clinical dose of lipids) dispersed in DMEM supplemented with 10% FBS, and the contents were treated for 15min at 37°C, 42°C and 45°C in water bath. For microscopic examinations, the plates were washed with PBS for 5 times and 1mL of 4% paraformaldehyde (PFA) were added

and kept for 15 minutes and washed with PBS for 5 times. The contents were incubated for 5 min with DAPI at 37°C in a 5% CO_2 atmosphere to stain the nuclei (blue). The cells were directly imaged on a matTek well plate under an Olympus IX81 confocal microscope using a 100 ms exposure time with the Green Fluorescent Protein filter (GFP, ex/em of 475/509) and a 50 ms exposure time with the DAPI (ex/em of 358/461) filter at 60x APO.

4.3.7 Quantification of liposome uptake by the macrophages

RAW 264.7macrophages were harvested and seeded with 2 mL of cell suspension at a rate of ($1x10^6$ cells/mL) onto 6 well cell culture plates. Prior to the experiment, the culture medium was discarded and the cells were incubated with fresh serum free DMEM medium containing 12uL liposome/ 2 mL for 15min at 37°C, 42°Cand 45°C, then the culture media was discarded, and the cells were recovered by tripsinization in 15-mL falcon tubes. The cells were centrifuged at 1000 rpm for 5 min toremove any non-phagocytosed liposomes, rinsed with 1x buffer, spun down, re-suspended in 100 µL of PBS, and subsequently the fluorescence intensity of was analyzed by FACS flow cytometry (BD FACS Aria, USA) with an excitation wavelength of 358/461 nm and analyzed with a 495/519 nm emission filter by counting 10,000 single cell events. Only the viable cells were gated for fluorescence analysis. The geometric mean fluorescence intensity of the cells was computed from the histogram plot calculated from triplicate data.

4.3.8 Cytokine gene expression analysis using Real Time PCR

Gene expression analysis were performed for pro-inflammatory (IL1-beta, TNF-α, IL6) and anti-inflammatory (IL10) cytokines.

RNA isolation and phenol chloroform RNA purification

Total RNA was extracted using TRIZOL (Invitrogen) according to the manufacturer's instructions. RNA concentration was measured using NanoDrop ND-100 followed by phenol chloroform RNA purification.

Reverse Transcription Polymerase Chain Reaction (RT-PCR). cDNA synthesis was performed using iScript Reverse Transcription Supermix for RT-qPCR and Real Time RT-PCR reaction was performed using 5 times diluted cDNA.

Quantitative Real-Time Reverse Transcription Polymerase Chain Reaction (qRT-PCR). Relative gene expression for IL1beta, TNFalpha, IL6 and IL10, as M1 and M2 specific cytokines was evaluated by qRT-PCR using SYBR green reagent (Eurogentec – qPCR Master Mix Plus for SYBR green) using AB applied Biosystem 7500 fast Real Time PCR instrument and indicated specific primers (Table 1). qRT-PCR data was analyzed by the $2^{(-\Delta\Delta CT)}$ method, using GAPDH as a reference gene.

Table 2.qRT-PCR primers sequences

qPCR primers	**Species**	**Sequences**
mGapdh-forward	***Mus musculus***	CATCACTGCCACCCAGAAGACTG
mGapdh-reverse	***Mus musculus***	ATGCCAGTGAGCTTCCCGTTCAG
mTnf- alpha-forward	***Mus musculus***	CACCACCATCAAGGACTCAA

mTnf-alpha-reverse	***Mus musculus***	AGGCAACCTGACCACTCTCC
mIl1-beta-forward	***Mus musculus***	TGGACCTTCCAGGATGAGGACA
mIl1-beta-reverse	***Mus musculus***	GTTCATCTCGGAGCCTGTAGTG
mIl6-forward	***Mus musculus***	ACAACCACGGCCTTCCCTACTT
mIl6-reverse	***Mus musculus***	CACGATTTCCCAGAGAACATGTG
mIl10-forward	***Mus musculus***	CGGGAAGACAATAACTGCACCC
mIl10-reverse	***Mus musculus***	CGGTTAGCAGTATGTTGTCCAGC

4.3.9. Analysis of CD86, CD206 and Cd11c Expression by Flow Cytometry

Treated RAW 264.7macrophages were washed and re-suspended in 1xPBS containing 2% fetal bovine serum. 100uL of cell suspension was incubated for 30 minutes with primary anti PE-CD86 antibody, primary anti Alexa Fluor 700-CD206 antibody and primary APC-CD11c antibody. Control isotype corresponding to each primary antibody served as control. Three washes with PBS containing 2% FBS were performed, and then cells were analyzed by flow cytometry with FACScalibur (BD Biosciences) at CD86, CD 206 and CD11C, respectively. Data was analyzed with FlowJo software, and represented as percentage CD86, CD206 and CD11c.

4.3.10. Cancer cell treatment with macrophage conditioned media

To evaluate if liposome/hyperthermia treatment of macrophages enhances cytotoxicity against cancer cells, $0.5*10^6$ B16F10 melanoma cells were incubated with 100 µL of serum containing media at 37°C for 24hours. The cells were then rinsed, and treated

with conditioned media from RAW 264.7 macrophages liposome and hyperthermia treatment and incubated for 24 hours at 37°C in a 5% CO_2 atmosphere. For comparison, control group without conditioned media with the same volume of serum free media were cultured similarly. End points were measurement of MTT assay, gene expression.

4.4. RESULTS

4.4.1 Physicochemical Characterization of Liposome

The hydrodynamic diameter, polydispersity index, and zeta-potential of liposomeswasabout 180 nm, 0.132 and -4.893 mV, respectively (Table 3).

Liposome	Size (nm)		Polydispersity		Zeta potential	
	mean	SD	mean	SD	mean	SD
LTSL	182.02	11.92	0.132	0.014	-4.893	4.128

Table 3 shows the hydrodynamic diameter, polydispersity index, and zeta potential values of LTSLs at room temperature (25 °C).

4.4.2. Cytotoxicity assessment of heat against macrophages

Co-incubation of RAW 264.7 cells with liposomes and hyperthermia did not result in significant killing compared to liposomes, the hyperthermia or the untreated control in the dose range of 10 μM at 37ºC ($p<0.05$). For all dose ranges, the absorbance was comparable or higher than the untreated control indicating a lack of toxicity in 6 hours

incubation post-hyperthermia treatment (Fig 10a). The toxicity at the indicated dose range was greater in 42ºC, 45ºC than 37ºC in presence of hyperthermia (~20%). In contrast, cells treated with liposome and 42ºC, 45ºC showed significant toxicity (~70%) in 24 hours post-hyperthermia treatment (Fig 10b) compared to untreated and normothermic samples in RAW 264.7 macrophage cells ($p<0.05$).

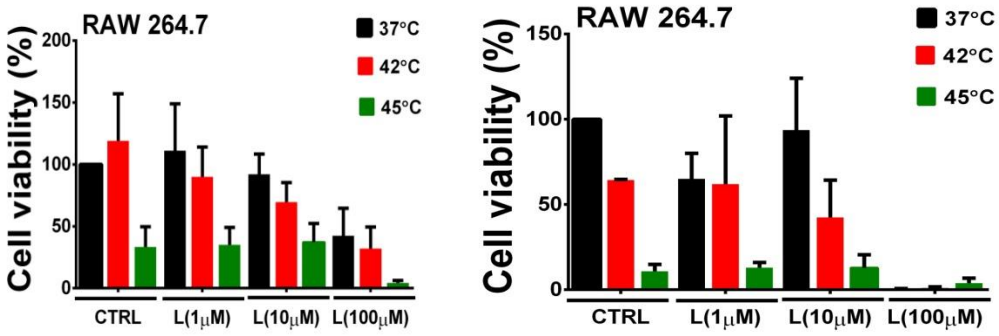

Figure 10: RAW 264.7 macrophage cells cytotoxicity assessment of heat against macrophages after 6 hours (Fig 10a) and 24 hours (Fig 10b) of post-hyperthermia using MTT assay. Data are expressed as Mean ± Standard deviation.

4.4.3. Cellular uptake of liposome uptake by macrophages

Liposomes were phagocytosed successfully upon incubation with the macrophage cells (Fig 11a). Based on the median fluorescence intensity of liposomes, the flow cytometry study suggested that uptake was significantly higher in the presence of heat (~ 80%)

compared to liposomes alone. Liposomes uptake by macrophages were shown in Fig 11b.

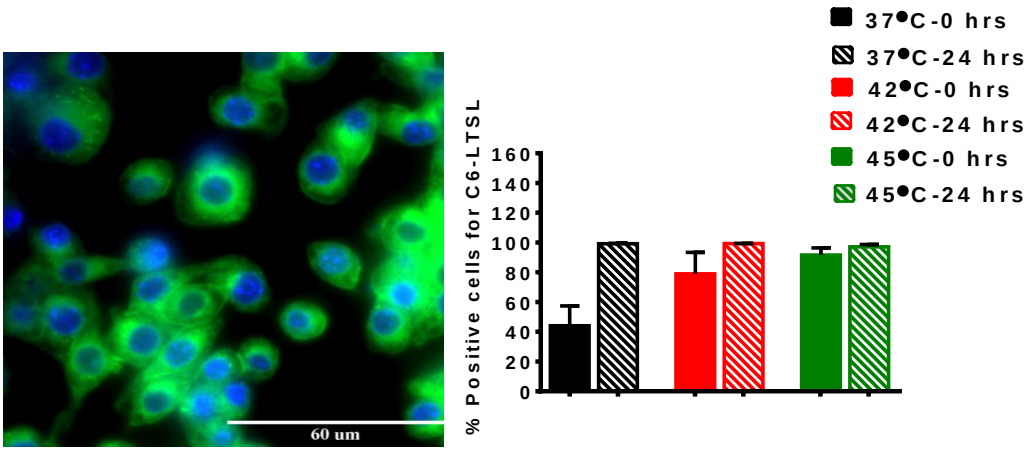

Figure 11: Cellular uptake of liposome by macrophage after 0 hours and 24 hours post treatment. Fig 11a-Confocal images of RAW 264.7 macrophages treated for 37ºC, 42ºC, 45ºC for 15 minutes with bare liposomes (LTSL). Cell nucleus is stained by using DAPI-stained (blue), and particles are stained by coumarin-6 (C6). Fig 11b-Flow cytometry graphs show % positive cells for C6-LTSL fluorescent values of three experiments ± SD. Liposomes with 42°C hyperthermia had a significantly higher uptake by RAW 264.7 cells than 37C hyperthermia. 37°C hyperthermia macrophage cells were used as controls.

4.4.4.Pro-Inflammatory Cytokine Gene Expression in RAW 246.7 macrophages.

At 6 hours of post-treatment RAW 264.macrophage cells treated with liposome and hyperthermia treatment showeda significant increase in pro-inflammatory cytokine expression (1500-2000 fold) by liposomes compared to untreated controls ($P<0.05$). Also, compared to liposome alone, the combination of liposome/hyperthermia achieved a greater increase in mRNA expression, suggesting that the liposome action is potentiated at 42°C (Fig. 12). In contrast, increase in the expression of IL-10 was relatively modest (~60-fold higher), indicating that real-time combination of heat/liposome has a more predominant pro-inflammatory phenotype inducing property in mouse macrophages. Interestingly, at 45°C the presence of liposome and hyperthermia increased anti-inflammatory cytokine expression (IL10; 200 fold) compare to 37°C or 42°C. However, this was also accompanied by an expression of TNF-alpha and IL-6 cytokines.

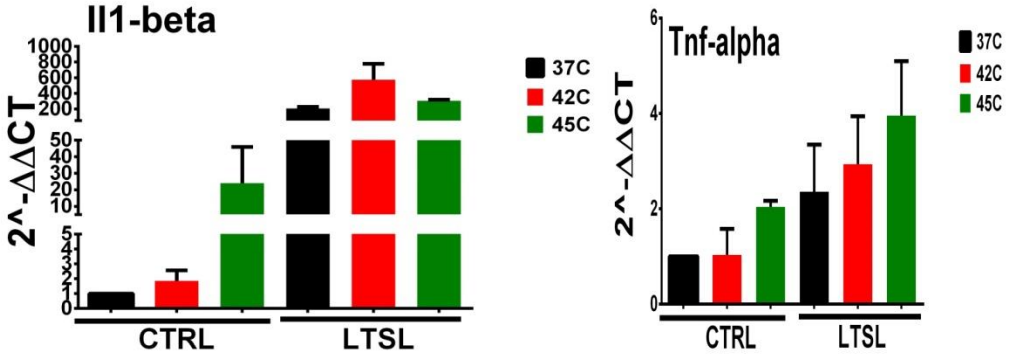

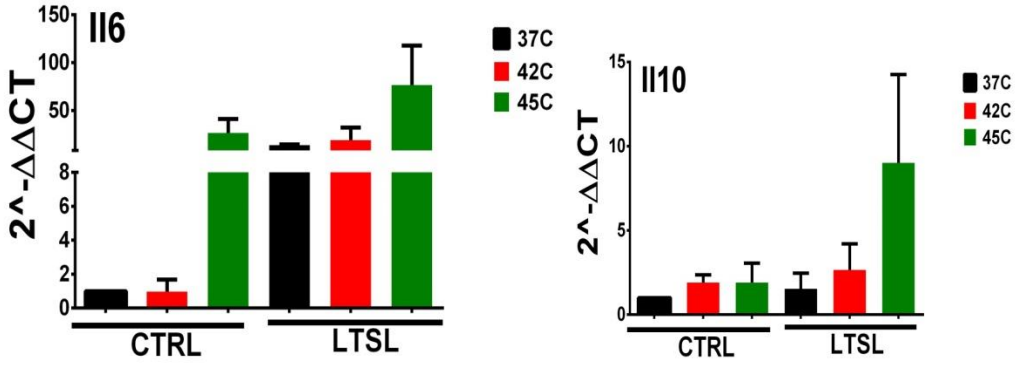

Fig 12: Cytokines such as IL-1(Fig 12a), TNF-alpha(Fig 12b),IL-6(Fig 12c),IL-10(Fig 12d) gene expression through Real Time PCR analysis on 6 hours post-treatment RAW 264.7 macrophage cells treated with liposome and hyperthermia treatment at 37°C, 42°C, 45°C.

At 24 hours of post-treated RAW 264.macrophages increase in the expression of IL-10 was relatively modest (~60-fold higher), indicating that real-time combination of heat/liposome has a more predominant pro-inflammatory phenotype inducing property in mouse macrophages. However, this was also accompanied by an expression of TNF-alpha and IL-6 cytokines.

4.4.5 Macrophage cell surface expression of CD86, CD206 and CD11c

The CD86 protein expression was 3%, 30% and 10% for control, heat and liposome + 42°C, liposome + 45°C respectively. In contrast, the expression of CD206 increased by 1% compared to untreated controls. These data are consistent with the gene expression results observed in the study described in Section 2.1.

When compare to the increased gene expression level of the pro-inflammatory cytokine, 6 hours after moderate hyperthermia associated with liposome treatment, the protein expression of CD86, CD206 and CD11c, cell surface associated markers were significant increased 24 hours post treatment (Fig 13a, Fig 13b, Fig 13c), suggesting a delay in cell surface associated markers expression compare to cytokine expression, after moderate hyperthermia treatment.

24 hours after liposome treatment at 42°C and 45°C macrophages adopted a combination of elongated, spindle-shaped morphology and rounded shaped morphology with elongated filopodia (Fig 13d). The highest morphology change, similar with a dendritic like cell shape, has been noticed in 24 hours after 42°C and 45°C treatment in the presence of liposome.

Furthermore, the change in cell morphology has been associated with a significant increase of CD11c surface marker 24 hours after 42°C and 45°C treatment in the presence of liposome, compare to the 42°C and 45°C, untreated cells (Fig 13e)

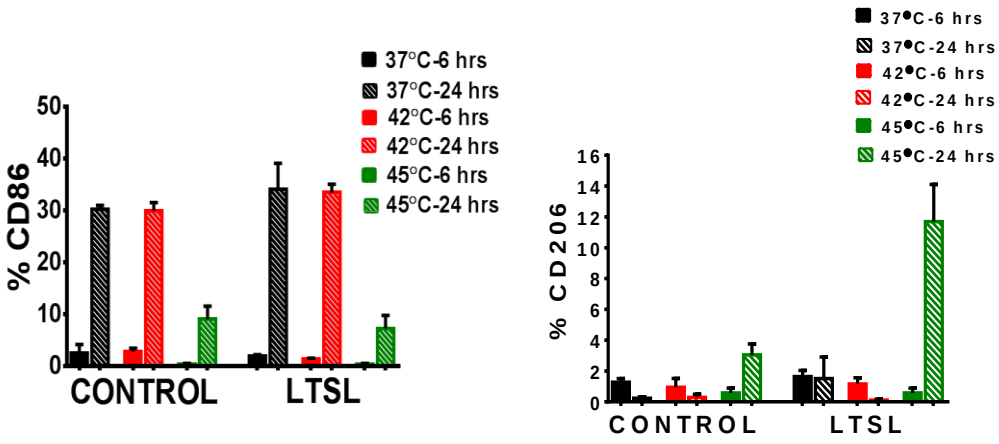

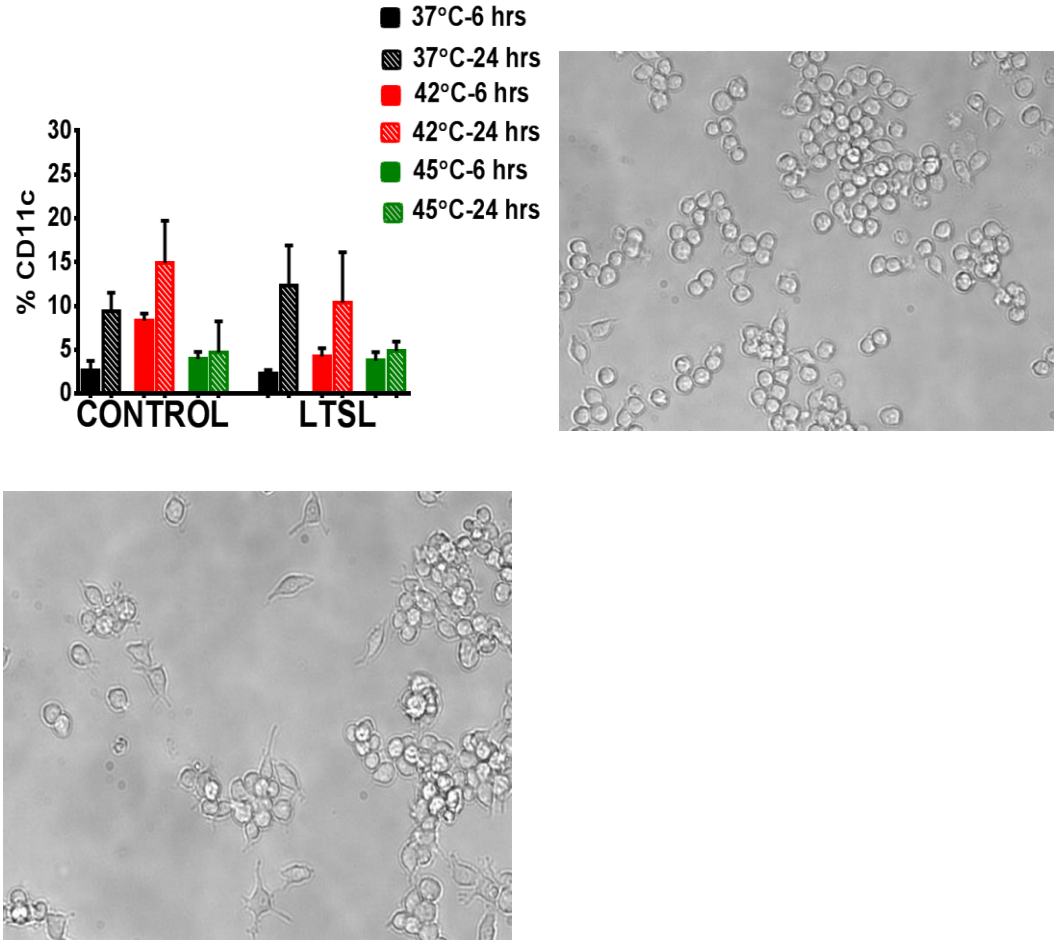

Figure 13: Assessment of M1 and M2 macrophages on cell surface by flow cytometry. LTSL and 37°C, 42°C, 45°C hyperthermia treated RAW 264.7 macrophages was stained for CD8, CD206 and CD11c. Number of macrophages that stained positively for each antigen were counted and expressed as percentage of CD86(Fig 13a), CD206(Fig 13b),CD11c(Fig 13c) macrophage cells and presence of dendritic phenotype(Fig 13e).

4.4.6 Cytotoxicity against melanoma cells

Co-incubation of B16F10 melanoma cells with conditioned media from RAW 264.7 macrophages treated with liposome and hyperthermia treatment after 24 hours did not result in significant killing compared to control ($p<0.05$). The cell viability was greater in 6 hours conditioned media liposome treatment (Fig 14a). In contrast, the cell death was significant ~30% in 24 hours conditioned media harvested from liposome treatment (Fig 14b) compared to untreated samples ($p<0.05$).

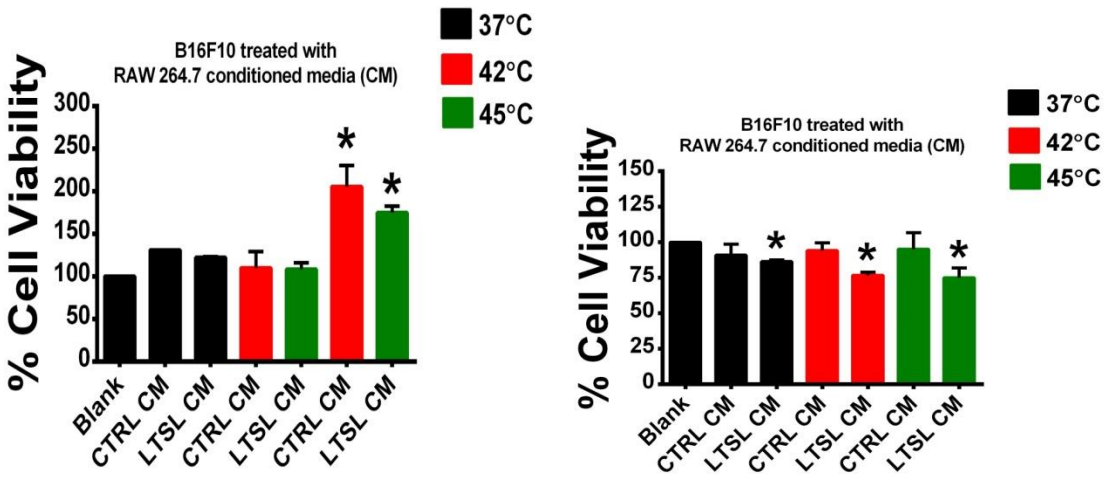

Figure 14: B16F10 cells cytotoxicity assessment of heat against macrophages after 6 hours (Fig 14a) and 24 hours (Fig 14b) of conditioned media from RAW 264.7 macrophages using MTT assay. Data are expressed as Mean ± Standard deviation.

4.5 Discussion

The tumor microenvironment is characterized by the presence of inflammatory cells such as macrophages and lymphocytes. These cells play an important role in carcinogenesis and suppression of antitumor immunity (Choi, Gyamfi et al. 2017). Of these, macrophages are the major component of leucocyte population and form approximately

50% of tumor mass (Vinogradov, Warren et al. 2014). Macrophages are typically hypothesized to originate from blood compartments, and exist in two distinct polarized phenotypes in tumors: M1 (classical activated) and M2 (alternatively activated pro-tumor)(Mantovani, Marchesi et al. 2017). Several preclinical and clinical studies have established that a high population of M2 macrophages in the tumors is associated with poor patient survival (Goswami, Ghosh et al. 2017). A variety of mechanisms triggers an M2 like phenotype in the tumor microenvironment. These include hypoxic and lactate microenvironment, a negative regulation by tumor necrosis factor (TNF), and the presence of anti-inflammatory cytokines driving M2 polarization (IL-4, IL10, and IL-13) (Kratochvill, Neale et al. 2015). In particular, the increased production of IL-10 correlates strongly with M2 specific cell surface expression of CD206 (Roszer 2015). These activation pathways impact chemotherapy delivery by affecting vascular leakage and also induce chemo resistance through the release of milk fat globule-epidermal growth factor 8 protein (MFG-E8) and subsequent activation of STAT3 to provides survival signals for tumor-initiating/cancer stem cells (CSCs) (De Palma and Lewis 2013). Thus, overcoming the M2 rich macrophage population in tumors can be a critical link in theimprovement of cancer chemo- and immuno-therapy.

One approach to overcome pro-humoral M2 phenotype can be by harnessing the high plasticity of macrophages to re-educate them towards a tumor-suppressive M1 phenotype using nanoparticles. Classically activated M1 macrophages secrete cytokines such as TNF, IL-1, IL-6, IL-8, and IL-12 to increase vascular permeability and recruitment of inflammatory cells in the tumor(Arango Duque and Descoteaux 2014). A

high M1/M2 ratio of macrophages directly induces cancer cell killing and is known to enhance survival in patients (e.g. ovarian tumors) (Zhang, He et al. 2014). To leverage these benefits, Wang et al. developed a tumor microenvironment-responsive poly (β-amino ester) encapsulated with IL-12 for passive accumulation in the tumor microenvironment. The releaseof IL-12 from the nanoparticles enhanced M1 specific cell surface expression and superior treatment responses (Wang, Lin et al. 2017). Similarly, Zanganeh et al. found that iron supplement ferumoxytol enhanced M1 phenotype via enhancement of caspase-3 and pro-inflammatory Th1 activity. This methodology also induced regression of subcutaneous adenocarcinomas in mice model (Zanganeh, Hutter et al. 2016). Based on these promising observations, we hypothesized that liposome/hyperthermia combination can synergistically modulate macrophage polarization dynamics. The use of liposomes is especially attractive since they are biodegradable and demonstrate a high degree of membrane stability that is essential for tumor accumulation (Meers, Neville et al. 2008). Liposomes are also adaptable for externally-triggered, localized release of drug payloads using hyperthermia (40-45ºC) (Negussie, Yarmolenko et al. 2010, Partanen, Yarmolenko et al. 2012, Ranjan, Jacobs et al. 2012). Hyperthermia alone can induce expression of higher levels of MICA, an NKG2D ligand for NK or $CD8^+$ T cells mediated tumor lysis (Toraya-Brown, Sheen et al. 2014). Thus, the combination of liposomes and hyperthermia potentially can result in a qualitatively new and integrated intervention that, if successful, can be translated to clinical application for both T-cell and macrophage modulated immunotherapy.

Nanoparticles are recognized as foreign particulate material and are phagocytosed by the tumor macrophages (Vinogradov, Warren et al. 2014). Typically, larger particles (100-1000μM) with low negative to positive charge demonstrate a more efficient endocytosis by the macrophages (Lee, Hwang et al. 2015). In this study, we aimed to attain a hydrodynamic size of 100-200 nm with low negative zeta potential for the liposomes to obtain endocytosis using the RAW264.7 murine macrophage cell line as a model. Confocal study confirmed that our formulation chemistry caused efficient cellular uptake in the endosomal and cytosolic compartment of the cells (Fig. 11a). Quantitative estimation of uptake rate by flow cytometry showed a relative greater (Fig. 11b) at 42ºC compared to 37ºC presumable due to the high metabolic competency of cells. As temperature increased from 42 to 45ºC, the uptake rates decreased probably due to poor survival of macrophages. This suggests that optimal temperature range for macrophage survival in tumors is quite narrow and require discreet control. An unexpected but surprising finding was the transition of macrophages towards a dendritic cell like phenotype at a higher temperature. This was evidenced by the high cell surface expression of CD11c and presence of dendritic phenotype (Fig. 13e). Studies are currently underway in the lab to understand the mechanism; however, the obtained data clearly suggest that the macrophages demonstrate a high temperature dependency in their plasticity. Additionally, the presence and intracellular uptake of liposomes dramatically impact gene expression to potentiate hyperthermia mediated responses. We also speculate that uptake of nanoparticles by the macrophages regardless of particle chemistry is the rate-limiting step for induction of cellular polarization. This is because our gene expression data with liposomes are in line with the previous

observation of Zanganeh et al. study that employed iron-oxide nanoparticles. In general, the main pro-inflammatory cytokines, IL1 beta, and TNF-α, were significantly increased and the specific anti-inflammatory markers, such as IL-10 were significantly decreased compared to untreated controls. Notably, the gene expression was not necessarily accompanied with cell surface expression; however, this process still resulted in significantly enhanced cancer cell cytotoxicity. In summary, nanoparticle induced responses are potentiated by heat induced cellular stress that causes differential gene expression, and this approach may serve as an important therapeutic component of macrophage-modulated cancer immunotherapies.

Our in vitro study has several limitations. The tumor microenvironment is much more complex *in vivo* due to the involvement of factors and signals mediated by the tumor cells and immunosuppressive immune cells and fibroblasts, which can impact macrophage polarization. In addition, immunosuppressors like myeloid-derived suppressor cells (MDSC), regulatory T cells, and factors like fibroblast growth factor, vascular endothelial growth factor, and tumor promoting cytokines may impact induction of M1 specific genes. The goal of our in vitro investigation was to specifically delineate the role of hyperthermia/nanoparticle therapy on macrophages. In future, we will perform timed analyses of T-cell, MDSCs, and cytokines in tumor and lymphoid organs like spleen and lymph nodes to assess such mechanisms in more detail. Another limitation of our work was a lack of long-lasting enhancement of the pro-inflammatory phenotype and anti-tumoral immune effect with heat. This is addressable clinically with more frequent treatments to induce greater regression.

In conclusion, our novel concept of liposome combined hyperthermia therapy of macrophages provides new insights on ways to spatially control the macrophage polarization and plasticity within tumors. To our best knowledge, the induction of macrophage polarization with liposomes has not been shown before, and their role in tumors has so far been largely limited to cell depot of drugs. Thus, we believe that elucidation of the alternative benefits of liposome with hyperthermia will eventually improve immunotherapies within the tumor microenvironment. This may lead to improved patient outcomes and thus advance clinical practice.

4.6 References

Allen, T. M. and P. R. Cullis (2013). "Liposomal drug delivery systems: from concept to clinical applications." Adv Drug Deliv Rev 65(1): 36-48.

Arango Duque, G. and A. Descoteaux (2014). "Macrophage cytokines: involvement in immunity and infectious diseases." Front Immunol 5: 491.

Arranja, A. G., V. Pathak, T. Lammers and Y. Shi (2016). "Tumor-targeted nanomedicines for cancer theranostics." Pharmacol Res.

Beatty, G. L., E. G. Chiorean, M. P. Fishman, B. Saboury, U. R. Teitelbaum, W. Sun, R. D. Huhn, W. Song, D. Li, L. L. Sharp, D. A. Torigian, P. J. O'Dwyer and R. H. Vonderheide (2011). "CD40 agonists alter tumor stroma and show efficacy against pancreatic carcinoma in mice and humans." Science 331(6024): 1612-1616.

Boissenot, T., A. Bordat, E. Fattal and N. Tsapis (2016). "Ultrasound-triggered drug delivery for cancer treatment using drug delivery systems: From theoretical considerations to practical applications." J Control Release 241: 144-163.

Choi, J., J. Gyamfi, H. Jang and J. S. Koo (2017). "The role of tumor-associated macrophage in breast cancer biology." Histol Histopathol: 11916.

De Palma, M. and C. E. Lewis (2013). "Macrophage regulation of tumor responses to anticancer therapies." Cancer Cell 23(3): 277-286.

Drummond, D. C., O. Meyer, K. Hong, D. B. Kirpotin and D. Papahadjopoulos (1999). "Optimizing liposomes for delivery of chemotherapeutic agents to solid tumors." Pharmacol Rev 51(4): 691-743.

Farkona, S., E. P. Diamandis and I. M. Blasutig (2016). "Cancer immunotherapy: the beginning of the end of cancer?" BMC Med 14: 73.

Gonzalez-Martin, A. and A. du Bois (2016). "Factors to consider and questions to ask in the management of recurrent ovarian cancer: a focus on the role of trabectedin + pegylated liposomal doxorubicin." Expert Rev Anticancer Ther 16(sup1): 3-10.

Goswami, K. K., T. Ghosh, S. Ghosh, M. Sarkar, A. Bose and R. Baral (2017). "Tumor promoting role of anti-tumor macrophages in tumor microenvironment." Cell Immunol 316: 1-10.

Kong, G., G. Anyarambhatla, W. P. Petros, R. D. Braun, O. M. Colvin, D. Needham and M. W. Dewhirst (2000). "Efficacy of liposomes and hyperthermia in a human tumor xenograft model: importance of triggered drug release." Cancer Res 60(24): 6950-6957.

Kratochvill, F., G. Neale, J. M. Haverkamp, L. A. Van de Velde, A. M. Smith, D. Kawauchi, J. McEvoy, M. F. Roussel, M. A. Dyer, J. E. Qualls and P. J. Murray (2015). "TNF Counterbalances the Emergence of M2 Tumor Macrophages." Cell Rep 12(11): 1902-1914.

Lee, J. S., S. Y. Hwang and E. K. Lee (2015). "Imaging-based analysis of liposome internalization to macrophage cells: Effects of liposome size and surface modification with PEG moiety." Colloids Surf B Biointerfaces 136: 786-790.

Mantovani, A., F. Marchesi, A. Malesci, L. Laghi and P. Allavena (2017). "Tumour-associated macrophages as treatment targets in oncology." Nat Rev Clin Oncol 14(7): 399-416.

Manzoor, A. A., L. H. Lindner, C. D. Landon, J. Y. Park, A. J. Simnick, M. R. Dreher, S. Das, G. Hanna, W. Park, A. Chilkoti, G. A. Koning, T. L. Ten Hagen, D. Needham and M. W. Dewhirst (2012). "Overcoming Limitations in Nanoparticle Drug Delivery: Triggered, Intravascular Release to Improve Drug Penetration into Tumors." Cancer Res.

Mayer, L. D., G. Dougherty, T. O. Harasym and M. B. Bally (1997). "The role of tumor-associated macrophages in the delivery of liposomal doxorubicin to solid murine fibrosarcoma tumors." J Pharmacol Exp Ther 280(3): 1406-1414.

Meers, P., M. Neville, V. Malinin, A. W. Scotto, G. Sardaryan, R. Kurumunda, C. Mackinson, G. James, S. Fisher and W. R. Perkins (2008). "Biofilm penetration, triggered release and in vivo activity of inhaled liposomal amikacin in chronic Pseudomonas aeruginosa lung infections." J Antimicrob Chemother 61(4): 859-868.

Mielgo, A. and M. C. Schmid (2013). "Impact of tumour associated macrophages in pancreatic cancer." BMB Rep 46(3): 131-138.

Negussie, A. H., P. S. Yarmolenko, A. Partanen, A. Ranjan, G. Jacobs, D. Woods, H. Bryant, D. Thomasson, M. W. Dewhirst, B. J. Wood and M. R. Dreher (2010). "Formulation and characterisation of magnetic resonance imageable thermally sensitive liposomes for use with magnetic resonance-guided high intensity focused ultrasound." Int J Hyperthermia 27(2): 140-155.

O'Brien, M. E., N. Wigler, M. Inbar, R. Rosso, E. Grischke, A. Santoro, R. Catane, D. G. Kieback, P. Tomczak, S. P. Ackland, F. Orlandi, L. Mellars, L. Alland, C. Tendler and C. B. C. S. Group (2004). "Reduced cardiotoxicity and comparable efficacy in a phase III trial of pegylated liposomal doxorubicin HCl (CAELYX/Doxil) versus conventional doxorubicin for first-line treatment of metastatic breast cancer." Ann Oncol 15(3): 440-449.

Ranjan, A., G. C. Jacobs, D. L. Woods, A. H. Negussie, A. Partanen, P. S. Yarmolenko, C. E. Gacchina, K. V. Sharma, V. Frenkel, B. J. Wood and M. R. Dreher (2012). "Image-

guided drug delivery with magnetic resonance guided high intensity focused ultrasound and temperature sensitive liposomes in a rabbit Vx2 tumor model." J Control Release 158(3): 487-494.

Roszer, T. (2015). "Understanding the Mysterious M2 Macrophage through Activation Markers and Effector Mechanisms." Mediators Inflamm 2015: 816460.

Senavirathna, L. K., R. Fernando, D. Maples, Y. Zheng, J. C. Polf and A. Ranjan (2013). "Tumor Spheroids as an In Vitro Model for Determining the Therapeutic Response to Proton Beam Radiotherapy and Thermally Sensitive Nanocarriers." Theranostics 3(9): 687-691.

Tagami, T., M. J. Ernsting and S. D. Li "Efficient tumor regression by a single and low dose treatment with a novel and enhanced formulation of thermosensitive liposomal doxorubicin." J Control Release 152(2): 303-309.

Toraya-Brown, S., M. R. Sheen, P. Zhang, L. Chen, J. R. Baird, E. Demidenko, M. J. Turk, P. J. Hoopes, J. R. Conejo-Garcia and S. Fiering (2014). "Local hyperthermia treatment of tumors induces CD8(+) T cell-mediated resistance against distal and secondary tumors." Nanomedicine 10(6): 1273-1285.

Vinogradov, S., G. Warren and X. Wei (2014). "Macrophages associated with tumors as potential targets and therapeutic intermediates." Nanomedicine (Lond) 9(5): 695-707.

Wang, Y., Y. X. Lin, S. L. Qiao, H. W. An, Y. Ma, Z. Y. Qiao, R. P. Rajapaksha and H. Wang (2017). "Polymeric nanoparticles promote macrophage reversal from M2 to M1 phenotypes in the tumor microenvironment." Biomaterials 112: 153-163.

Zanganeh, S., G. Hutter, R. Spitler, O. Lenkov, M. Mahmoudi, A. Shaw, J. S. Pajarinen, H. Nejadnik, S. Goodman, M. Moseley, L. M. Coussens and H. E. Daldrup-Link (2016). "Iron oxide nanoparticles inhibit tumour growth by inducing pro-inflammatory macrophage polarization in tumour tissues." Nat Nanotechnol 11(11): 986-994.

Zhang, M., Y. He, X. Sun, Q. Li, W. Wang, A. Zhao and W. Di (2014). "A high M1/M2 ratio of tumor-associated macrophages is associated with extended survival in ovarian cancer patients." J Ovarian Res 7: 19.

Zhou, S., T. Zhang, B. Peng, X. Luo, X. Liu, L. Hu, Y. Liu, D. Di, Y. Song and Y. Deng (2017). "Targeted delivery of epirubicin to tumor-associated macrophages by sialic acid-cholesterol conjugate modified liposomes with improved antitumor activity." Int J Pharm 523(1): 203-216.

REFERENCES

Allen, T. M. and P. R. Cullis (2013). "Liposomal drug delivery systems: from concept to clinical applications." Adv Drug Deliv Rev 65(1): 36-48.

Arango Duque, G. and A. Descoteaux (2014). "Macrophage cytokines: involvement in immunity and infectious diseases." Front Immunol 5: 491.

Arranja, A. G., V. Pathak, T. Lammers and Y. Shi (2016). "Tumor-targeted nanomedicines for cancer theranostics." Pharmacol Res.

Bandyopadhyay, S., T. J. Quinn, L. Scandiuzzi, I. Basu, A. Partanen, W. A. Tome, F. Macian and C. Guha (2016). "Low-Intensity Focused Ultrasound Induces Reversal of Tumor-Induced T Cell Tolerance and Prevents Immune Escape." J Immunol 196(4): 1964-1976.

Beatty, G. L., E. G. Chiorean, M. P. Fishman, B. Saboury, U. R. Teitelbaum, W. Sun, R. D. Huhn, W. Song, D. Li, L. L. Sharp, D. A. Torigian, P. J. O'Dwyer and R. H. Vonderheide (2011). "CD40 agonists alter tumor stroma and show efficacy against pancreatic carcinoma in mice and humans." Science 331(6024): 1612-1616.

Blattman, J. N. and P. D. Greenberg (2004). "Cancer immunotherapy: a treatment for the masses." Science 305(5681): 200-205.

Boissenot, T., A. Bordat, E. Fattal and N. Tsapis (2016). "Ultrasound-triggered drug delivery for cancer treatment using drug delivery systems: From theoretical considerations to practical applications." J Control Release 241: 144-163.

Ciardiello, F., R. Caputo, R. Bianco, V. Damiano, G. Pomatico, S. De Placido, A. R. Bianco and G. Tortora (2000). "Antitumor Effect and Potentiation of Cytotoxic Drugs Activity in Human Cancer Cells by ZD-1839 (Iressa), an Epidermal Growth Factor Receptor-selective Tyrosine Kinase Inhibitor." Clinical Cancer Research 6(5): 2053-2063.

Choi, J., J. Gyamfi, H. Jang and J. S. Koo (2017). "The role of tumor-associated macrophage in breast cancer biology." Histol Histopathol: 11916.

Clay, T. M., A. C. Hobeika, P. J. Mosca, H. K. Lyerly and M. A. Morse (2001). "Assays for Monitoring Cellular Immune Responses to Active Immunotherapy of Cancer." Clinical Cancer Research 7(5): 1127-1135.

Deng, J., Y. Zhang, J. Feng and F. Wu (2010). "Dendritic Cells Loaded with Ultrasound-Ablated Tumour Induce in vivo Specific Antitumour Immune Responses." Ultrasound in Medicine & Biology 36(3): 441-448.

De Palma, M. and C. E. Lewis (2013). "Macrophage regulation of tumor responses to anticancer therapies." Cancer Cell 23(3): 277-286.

Drummond, D. C., O. Meyer, K. Hong, D. B. Kirpotin and D. Papahadjopoulos (1999). "Optimizing liposomes for delivery of chemotherapeutic agents to solid tumors." Pharmacol Rev 51(4): 691-743.

Engleman, E. G. and L. Fong (2003). "Induction of immunity to tumor-associated antigens following dendritic cell vaccination of cancer patients." Clin Immunol 106(1): 10-15.

Farkona, S., E. P. Diamandis and I. M. Blasutig (2016). "Cancer immunotherapy: the beginning of the end of cancer?" BMC Med 14: 73.

Gonzalez-Martin, A. and A. du Bois (2016). "Factors to consider and questions to ask in the management of recurrent ovarian cancer: a focus on the role of trabectedin + pegylated liposomal doxorubicin." Expert Rev Anticancer Ther 16(sup1): 3-10.

Goswami, K. K., T. Ghosh, S. Ghosh, M. Sarkar, A. Bose and R. Baral (2017). "Tumor promoting role of anti-tumor macrophages in tumor microenvironment." Cell Immunol 316: 1-10.

Hoos, A., A. M. Eggermont, S. Janetzki, F. S. Hodi, R. Ibrahim, A. Anderson, R. Humphrey, B. Blumenstein, L. Old and J. Wolchok (2010). "Improved endpoints for cancer immunotherapy trials." J Natl Cancer Inst 102(18): 1388-1397.

Hu, Z., X. Y. Yang, Y. Liu, G. N. Sankin, E. C. Pua, M. A. Morse, H. K. Lyerly, T. M. Clay and P. Zhong (2007). "Investigation of HIFU-induced anti-tumor immunity in a murine tumor model." Journal of Translational Medicine 5: 34-34.

Husseini, G. A. and W. G. Pitt (2008). "The use of ultrasound and micelles in cancer treatment." J Nanosci Nanotechnol 8(5): 2205-2215.

Inoue, S., Y. Setoyama and A. Odaka (2014). "Doxorubicin treatment induces tumor cell death followed by immunomodulation in a murine neuroblastoma model." Experimental and Therapeutic Medicine 7(3): 703-708.

Kim, S. J. and B. Diamond (2007). "Generation and maturation of bone marrow-derived DCs under serum-free conditions." J Immunol Methods 323(2): 101-108.

Kong, G., G. Anyarambhatla, W. P. Petros, R. D. Braun, O. M. Colvin, D. Needham and M. W. Dewhirst (2000). "Efficacy of liposomes and hyperthermia in a human tumor xenograft model: importance of triggered drug release." Cancer Res 60(24): 6950-6957.

Kratochvill, F., G. Neale, J. M. Haverkamp, L. A. Van de Velde, A. M. Smith, D. Kawauchi, J. McEvoy, M. F. Roussel, M. A. Dyer, J. E. Qualls and P. J. Murray (2015). "TNFCounterbalances the Emergence of M2 Tumor Macrophages." Cell Rep 12(11): 1902-1914.

Lee, J. S., S. Y. Hwang and E. K. Lee (2015). "Imaging-based analysis of liposome internalization to macrophage cells: Effects of liposome size and surface modification with PEG moiety." Colloids Surf B Biointerfaces 136: 786-790.

Liu, H. L., H. Y. Hsieh, L. A. Lu, C. W. Kang, M. F. Wu and C. Y. Lin (2012). "Low-pressure pulsed focused ultrasound with microbubbles promotes an anticancer immunological response." J Transl Med 10: 221.

Madaan, A., R. Verma, A. T. Singh, S. K. Jain and M. Jaggi (2014). "A stepwise procedure for isolation of murine bone marrow and generation of dendritic cells." Journal of Biological Methods 1(1).

Maples, D., K. McLean, K. Sahoo, R. Newhardt, P. Venkatesan, B. Wood and A. Ranjan (2015). "Synthesis and characterisation of ultrasound imageable heat-sensitive liposomes for HIFU therapy." Int J Hyperthermia 31(6): 674-685.

Mantovani, A., F. Marchesi, A. Malesci, L. Laghi and P. Allavena (2017). "Tumour-associated macrophages as treatment targets in oncology." Nat Rev Clin Oncol 14(7): 399-416.

Manzoor, A. A., L. H. Lindner, C. D. Landon, J. Y. Park, A. J. Simnick, M. R. Dreher, S. Das, G. Hanna, W. Park, A. Chilkoti, G. A. Koning, T. L. Ten Hagen, D. Needham and M. W. Dewhirst (2012). "Overcoming Limitations in Nanoparticle Drug Delivery:

Triggered, Intravascular Release to Improve Drug Penetration into Tumors." Cancer Res.

Mayer, L. D., G. Dougherty, T. O. Harasym and M. B. Bally (1997). "The role of tumor-associated macrophages in the delivery of liposomal doxorubicin to solid murine fibrosarcoma tumors." J Pharmacol Exp Ther 280(3): 1406-1414.

Meers, P., M. Neville, V. Malinin, A. W. Scotto, G. Sardaryan, R. Kurumunda, C. Mackinson, G. James, S. Fisher and W. R. Perkins (2008). "Biofilm penetration, triggered release and in vivo activity of inhaled liposomal amikacin in chronic Pseudomonas aeruginosa lung infections." J Antimicrob Chemother 61(4): 859-868.

Mellman, I., G. Coukos and G. Dranoff (2011). "Cancer immunotherapy comes of age." Nature 480(7378): 480-489.

Merad, M., T. Sugie, E. G. Engleman and L. Fong (2002). "In vivo manipulation of dendritic cells to induce therapeutic immunity." Blood 99(5): 1676-1682.

Mielgo, A. and M. C. Schmid (2013). "Impact of tumour associated macrophages in pancreatic cancer." BMB Rep 46(3): 131-138.

Negussie, A. H., P. S. Yarmolenko, A. Partanen, A. Ranjan, G. Jacobs, D. Woods, H. Bryant, D. Thomasson, M. W. Dewhirst, B. J. Wood and M. R. Dreher (2010). "Formulation and characterisation of magnetic resonance imageable thermally sensitive

liposomes for use with magnetic resonance-guided high intensity focused ultrasound." Int J Hyperthermia 27(2): 140-155.

O'Brien, M. E., N. Wigler, M. Inbar, R. Rosso, E. Grischke, A. Santoro, R. Catane, D. G. Kieback, P. Tomczak, S. P. Ackland, F. Orlandi, L. Mellars, L. Alland, C. Tendler and C. B. C. S. Group (2004). "Reduced cardiotoxicity and comparable efficacy in a phase III trial of pegylated liposomal doxorubicin HCl (CAELYX/Doxil) versus conventional doxorubicin for first-line treatment of metastatic breast cancer." Ann Oncol 15(3): 440-449.

Pei, Q., J. Pan, X. Ding, J. Wang, X. Zou and Y. Lv (2015). "Gemcitabine sensitizes pancreatic cancer cells to the CTLs antitumor response induced by BCG-stimulated dendritic cells via a Fas-dependent pathway." Pancreatology 15(3): 233-239.

Perica, K., J. C. Varela, M. Oelke and J. Schneck (2015). "Adoptive T cell immunotherapy for cancer." Rambam Maimonides Med J 6(1): e0004.

Ranjan, A., G. C. Jacobs, D. L. Woods, A. H. Negussie, A. Partanen, P. S. Yarmolenko, C. E. Gacchina, K. V. Sharma, V. Frenkel, B. J. Wood and M. R. Dreher (2012). "Image-guided drug delivery with magnetic resonance guided high intensity focused ultrasound and temperature sensitive liposomes in a rabbit Vx2 tumor model." J Control Release 158(3): 487-494.

Rosenberg, S. A. (1999). "A new era for cancer immunotherapy based on the genes that encode cancer antigens." Immunity 10(3): 281-287.

Roszer, T. (2015). "Understanding the Mysterious M2 Macrophage through Activation Markers and Effector Mechanisms." Mediators Inflamm 2015: 816460.

Saha, S., P. Bhanja, A. Partanen, W. Zhang, L. Liu, W. Tomé and C. Guha (2014). "Low intensity focused ultrasound (LOFU) modulates unfolded protein response and sensitizes prostate cancer to 17AAG." Oncoscience 1(6): 434-445.

Schuler, G., B. Schuler-Thurner and R. M. Steinman (2003). "The use of dendritic cells in cancer immunotherapy." Curr Opin Immunol 15(2): 138-147.

Senavirathna, L. K., R. Fernando, D. Maples, Y. Zheng, J. C. Polf and A. Ranjan (2013). "Tumor Spheroids as an In Vitro Model for Determining the Therapeutic Response to Proton Beam Radiotherapy and Thermally Sensitive Nanocarriers." Theranostics 3(9): 687-691.

Suzuki, R., Y. Oda, N. Utoguchi, E. Namai, Y. Taira, N. Okada, N. Kadowaki, T. Kodama, K. Tachibana and K. Maruyama (2009). "A novel strategy utilizing ultrasound for antigen delivery in dendritic cell-based cancer immunotherapy." Journal of Controlled Release 133(3): 198-205.

Tagami, T., M. J. Ernsting and S. D. Li "Efficient tumor regression by a single and low dose treatment with a novel and enhanced formulation of thermosensitive liposomal doxorubicin." J Control Release 152(2): 303-309.

Tan, Y. F., C. F. Leong and S. K. Cheong (2010). "Observation of dendritic cell morphology under light, phase-contrast or confocal laser scanning microscopy." Malays J Pathol 32(2): 97-102.

Tardoski, S., J. Ngo, E. Gineyts, J. P. Roux, P. Clezardin and D. Melodelima (2015). "Low-intensity continuous ultrasound triggers effective bisphosphonate anticancer activity in breast cancer." Sci Rep 5: 16354.

Toraya-Brown, S., M. R. Sheen, P. Zhang, L. Chen, J. R. Baird, E. Demidenko, M. J. Turk, P. J. Hoopes, J. R. Conejo-Garcia and S. Fiering (2014). "Local hyperthermia treatment of tumors induces CD8(+) T cell-mediated resistance against distal and secondary tumors." Nanomedicine 10(6): 1273-1285.

Vanneman, M. and G. Dranoff (2012). "Combining immunotherapy and targeted therapies in cancer treatment." Nat Rev Cancer 12(4): 237-251.

Vinogradov, S., G. Warren and X. Wei (2014). "Macrophages associated with tumors as potential targets and therapeutic intermediates." Nanomedicine (Lond) 9(5): 695-707.

Wang, Y., Y. X. Lin, S. L. Qiao, H. W. An, Y. Ma, Z. Y. Qiao, R. P. Rajapaksha and H. Wang (2017). "Polymeric nanoparticles promote macrophage reversal from M2 to M1 phenotypes in the tumor microenvironment." Biomaterials 112: 153-163.

Watanabe, M., N. Kakuta, K. Mabuchi and Y. Yamada (2005). "Micro-thermocouple probe for measurement of cellular thermal responses." Conf Proc IEEE Eng Med Biol Soc 5: 4858-4861.

Wu, F., Z.-B. Wang, P. Lu, Z.-L. Xu, W.-Z. Chen, H. Zhu and C.-B. Jin (2004). "Activated anti-tumor immunity in cancer patients after high intensity focused ultrasound ablation." Ultrasound in Medicine & Biology 30(9): 1217-1222.

Yang, R., C. R. Reilly, F. J. Rescorla, N. T. Sanghvi, F. J. Fry, T. D. Franklin and J. L. Grosfeld (1992). "Papers presented at the 22nd Annual Meeting of the American Pediatric Surgical AssociationEffects of high-intensity focused ultrasound in the treatment of experimental neuroblastoma." Journal of Pediatric Surgery 27(2): 246-251.

Zhang, H.-G., K. Mehta, P. Cohen and C. Guha (2008). "Hyperthermia on immune regulation: A temperature's story." Cancer Letters 271(2): 191-204.

Zhang, M., Y. He, X. Sun, Q. Li, W. Wang, A. Zhao and W. Di (2014). "A high M1/M2 ratio of tumor-associated macrophages is associated with extended survival in ovarian cancer patients." J Ovarian Res 7: 19.

Zanganeh, S., G. Hutter, R. Spitler, O. Lenkov, M. Mahmoudi, A. Shaw, J. S. Pajarinen, H. Nejadnik, S. Goodman, M. Moseley, L. M. Coussens and H. E. Daldrup-Link (2016). "Iron oxide nanoparticles inhibit tumour growth by inducing pro-inflammatory macrophage polarization in tumour tissues." Nat Nanotechnol 11(11): 986-994.

Zhou, Q., X.-Q. Zhu, J. Zhang, Z.-L. Xu, P. Lu and F. Wu (2008). "Changes in Circulating Immunosuppressive Cytokine Levels of Cancer Patients After High Intensity Focused Ultrasound Treatment." Ultrasound in Medicine & Biology 34(1): 81-87.

Zhou, S., T. Zhang, B. Peng, X. Luo, X. Liu, L. Hu, Y. Liu, D. Di, Y. Song and Y. Deng (2017). "Targeted delivery of epirubicin to tumor-associated macrophages by sialic acid-cholesterol conjugate modified liposomes with improved antitumor activity." Int J Pharm 523(1): 203-216.

VITA

RamasamySelvarani

Candidate for the Degree of

Master of Science

Thesis: TUMOR IMMUNOMODULATION OF FOCUSED ULTRASOUND AND BUBBLE LIPOSOMES THERAPY

Major Field: Veterinary Biomedical Sciences

Biographical:

Education:

Completed the requirements for the Master of Sciencein Veterinary Biomedical Sciences at Oklahoma State University, Stillwater, Oklahoma in December, 2017.

Completed the requirements for the Bachelor of Veterinary Science in Veterinary Medicine at MVC, TANUVAS University, Chennai, Tamilnadu, India in 2009.

Experience:

Professional Memberships: